



Comparative analysis of the shape and size of the middle ear cavity of turtles reveals no correlation with habitat ecology

Christian Foth,¹  Serjoscha W. Evers,^{1,2} Walter G. Joyce,¹ Virginie S. Volpato¹ and Roger B. J. Benson² 

¹Department of Geosciences, University of Fribourg, Fribourg, Switzerland

²Department of Earth Sciences, University of Oxford, Oxford, UK

Abstract

The middle ear of turtles differs from other reptiles in being separated into two distinct compartments. Several ideas have been proposed as to why the middle ear is compartmentalized in turtles, most suggesting a relationship with underwater hearing. Extant turtle species span fully marine to strictly terrestrial habitats, and ecomorphological hypotheses of turtle hearing predict that this should correlate with variation in the structure of the middle ear due to differences in the fluid properties of water and air. We investigate the shape and size of the air-filled middle ear cavity of 56 extant turtles using 3D data and phylogenetic comparative analysis to test for correlations between habitat preferences and the shape and size of the middle ear cavity. Only weak correlations are found between middle ear cavity size and ecology, with aquatic taxa having proportionally smaller cavity volumes. The middle ear cavity of turtles exhibits high shape diversity among species, but we found no relationship between this shape variation and ecology. Surprisingly, the estimated acoustic transformer ratio, a key functional parameter of impedance-matching ears in vertebrates, also shows no relation to habitat preferences (aquatic/terrestrial) in turtles. We suggest that middle ear cavity shape may be controlled by factors unrelated to hearing, such as the spatial demands of surrounding cranial structures. A review of the fossil record suggests that the modern turtle ear evolved during the Early to Middle Jurassic in stem turtles broadly adapted to freshwater and terrestrial settings. This, combined with our finding that evolutionary transitions between habitats caused only weak evolutionary changes in middle ear structure, suggests that tympanic hearing in turtles evolved as a compromise between subaerial and underwater hearing.

Key words: hearing; middle ear; morphometric measurements; spherical harmonics; Testudines.

Introduction

The ear is one of the primary sensory organs of tetrapods and has two main functions: the perception of sound and the coordination of gaze control, movement, and balance (e.g. Spoor & Zonneveld, 1998; Kardong, 2012; Ekdale, 2016). Following the transition from water to land, the ear of early tetrapods underwent a major transformation because of different demands placed on hearing in air as compared with water (Clack & Anderson, 2017). As the impedance of air is substantially lower than that of the endolymph that fills the inner ear, the first land-going tetrapods were probably only able to perceive low frequency

sounds in air because most mechanical energy of high-frequency sounds would have been deflected at the surface of the skull and not transferred to the inner ear (Clack, 1998, 2002; Hetherington, 2008). Four structures in combination are thought to be diagnostic for the acquisition of an impedance-matching ear that allows hearing higher frequency sounds in air: (1) a tympanum, i.e. a flexible, external membrane that vibrates in response to airborne sound waves, (2) an air-filled middle ear, which houses the hearing ossicles, (3) light-weight ear ossicles, typically the columella (=stapes), which transfer vibrations from the tympanum to the inner ear, and (4) the round window or analogue as a pressure relief system within the inner ear.

Fossils demonstrate the independent evolutionary origin of impedance-matching ears in several tetrapod lineages (Lombard & Bolt, 1979; Clack, 1998; Müller & Tsuji, 2007; Luo et al. 2016; Sobral et al. 2016; Evans, 2017), although functional and phylogenetic uncertainties make it currently difficult to quantify the exact number of independent

Correspondence

Christian Foth, Department of Geosciences, University of Fribourg, 1700 Fribourg, Switzerland. E: christian.foth@gmx.net

Accepted for publication 10 July 2019

events. It is nevertheless clear from phylogenetic character optimization that the four structures listed above evolved fully independently from one another in the amphibian, mammalian and reptilian lineages, in some instances using non-homologous structures (Clack, 1998, 2002; Sobral et al. 2016). The independent evolutionary origins of tympanic hearing in these clades are characterized by differences in the structure and homology of key components (e.g. Manley, 1972; Henson, 1974; Allin, 1975; Saunders et al. 2000; Luo et al. 2016).

The middle ear of turtles in general resembles that of most other reptiles in possessing a tympanum, an air-filled middle ear cavity and the osseous columella, which articulates laterally with the tympanic membrane via the cartilaginous extracolumella (Hetherington, 2008; Kardong, 2012). The columella is a thin rod that is medially expanded to a disk-like stapedial footplate that articulates with the fenestra ovalis. As in some other reptiles, the columella and extracolumella together form a relatively straight acoustic chain that lacks a complex lever system that could further amplify the forces acting upon the inner ear fluids. The extracolumella itself is a simple element that broadens toward the tympanic membrane but lacks additional processes (Olson, 1966). Therefore, the middle ear of turtles relies almost entirely on the ratio of the tympanic to oval window (fenestra ovalis) areas to facilitate sound energy transmission (Hetherington, 2008). The differences in area

between the tympanic membrane and the fenestra ovalis allow for the amplification of sound energy received at the tympanic membrane, accounting for the impedance difference of air and endolymph (Henson, 1974; Nummela & Thewissen, 2008).

In contrast to other reptiles, the middle ear cavity of turtles does not directly extend to the oval window, but is instead separated into two compartments (Fig. 1) by an osteological constriction called the incisura columellae auris (Gaffney, 1979). The lateral compartment of the middle ear, the middle ear cavity, is an air-filled space on the lateral surface of the skull that is predominantly formed by the quadrate. The medial compartment, on the other hand, is part of a large cavity called the cavum acustico-jugulare, through which many neurovascular vessels traverse, typically the jugular vein, lateral head vein and stapedial artery, mandibular artery and the cranial nerves IX–XI (e.g. Gaffney, 1979). Of the structures housed within the cavum acustico-jugulare, the pericapsular recess is particularly relevant for the auditory system (Henson, 1974; Wever, 1978; Hetherington, 2008). Turtles lack a round window (sometimes called fenestra pseudorotunda, but see Clack et al. 2016), which serves as a pressure relief for inner ear fluid motion induced by movements of the columella in most reptiles (Henson, 1974; Wever, 1978; Hetherington, 2008). Instead, the pericapsular recess forms a fluid-filled, ring-shaped structure that extends from the inner ear labyrinth

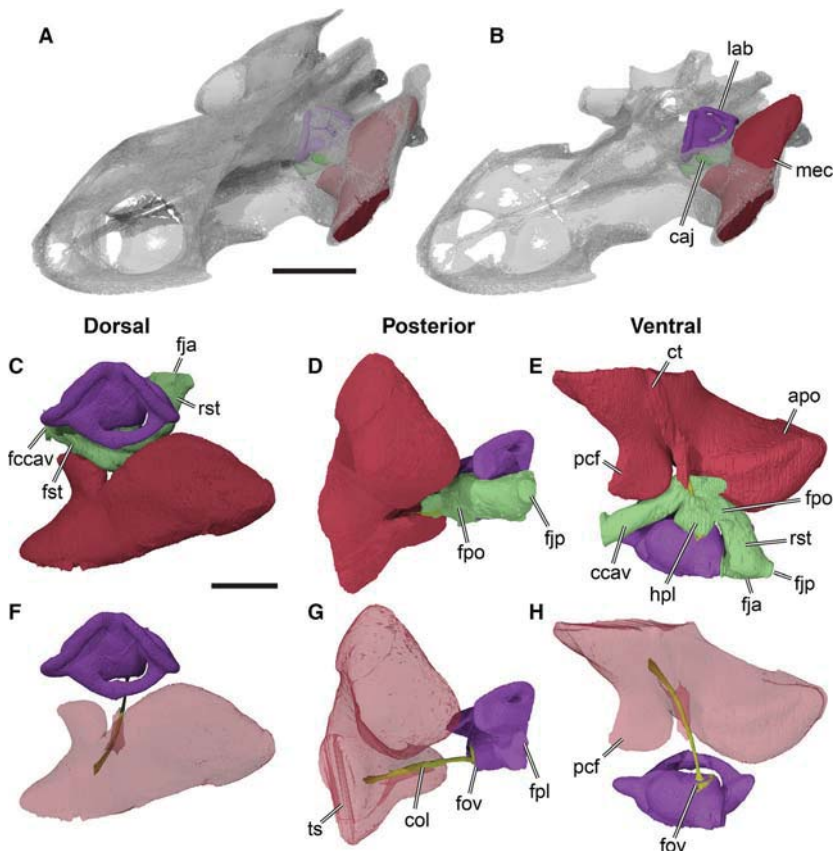


Fig. 1 Overview of turtle ear anatomy, exemplified by digital models of *Chelodina oblonga* (NHMUK 64.12.22). (A) 3D rendering of a transparent cranium in left lateral and anterodorsal view. (B) As (A), but with cranium horizontally sectioned to better show position of major ear structures. (C–E) Solid 3D renderings of the endocasts of the endosseous labyrinth, the cavum acustico-jugulare and the middle ear cavity (cavum tympani and recesses) in different views. (F–H) Solid 3D rendering of the endosseous labyrinth and columella, transparent rendering of the middle ear cavity to show the stapedial pathway of the tympanic ear. Scale bars: (A,B) 10 mm, (C–H) 5 mm. apo, antrum postoticum; caj, cavum acustico-jugulare; ccav, canalis cavernosus; col, columella; ct, cavum tympani; fccav, foramen cavernosum; fja, foramen jugulare anterius; fjp, foramen jugulare posterius; fov, fenestra ovalis; fpl, fenestra perilymphatica; fpo, fenestra postotica; fst, foramen stapedio-temporale; hpl, hiatus postlagenum; lab, endosseous labyrinth; mec, middle ear chamber; pcf, precolumellar fossa; rst, recessus scalae tympani; ts, tympanum surface.

through the fenestra perilymphatica, continues through the recessus scalae tympani, and then reconnects to the fenestra ovalis, thereby establishing a continuous, re-entrant fluid flow system around the footplate of the columella (Wever, 1978). Thus, sound wave energy, rather than being released at a release window, dissipates within the pericap-sular recess (Hetherington, 2008).

The majority of the middle ear cavity of turtles is comprised of a funnel-shaped space, the cavum tympani, that is mostly formed by the quadrate, but many groups of turtles possess diverticula that extend into the quadrate or the squamosal (Fig. 2). The largest of these diverticula are the antrum postoticum, a posterior expansion into the squamosal, and the precolumellar fossa, an anteromedial expansion into the quadrate (Gaffney, 1979; Gaffney et al. 2006). Although the term middle ear cavity is a misnomer, as it only represents the lateral portion of the middle ear, we here retain usage of this term, as it is consistently used in the literature.

Several ideas have been proposed as to why the tympanic middle ear of turtles is compartmentalized, and why the lateral part (i.e. the middle ear cavity) is filled with air. Some

studies interpret this morphology to be an aquatic specialization functioning as a resonance chamber, based on empirical data of airborne and underwater hearing sensitivity of the freshwater aquatic turtle *Trachemys scripta* (Christensen-Dalsgaard et al. 2012; Willis et al. 2013). Another explanation is that this air-filled cavity improves low-frequency sound conduction by decreasing the stiffness reactance, which determines middle ear impedance at low frequencies (Moore, 1981; Saunders et al. 2000). Alternatively, improved underwater sound localization or prevention of a middle ear cavity collapse from exposition to high pressures during diving have been proposed (Hetherington, 2008). In any case, most hypotheses for explaining the compartmentalization of the turtle middle ear imply some relationship to underwater hearing (Hetherington, 2008).

If the peculiar middle ear anatomy of turtles was the result of ecological adaptation to certain habitats, one would expect to see shape differences according to ecological gradients. These differences could relate to many distinct aspects of the osteology and configuration of the turtle ear, including the tympanic-to-oval window area ratio (which could be expected to be reduced in

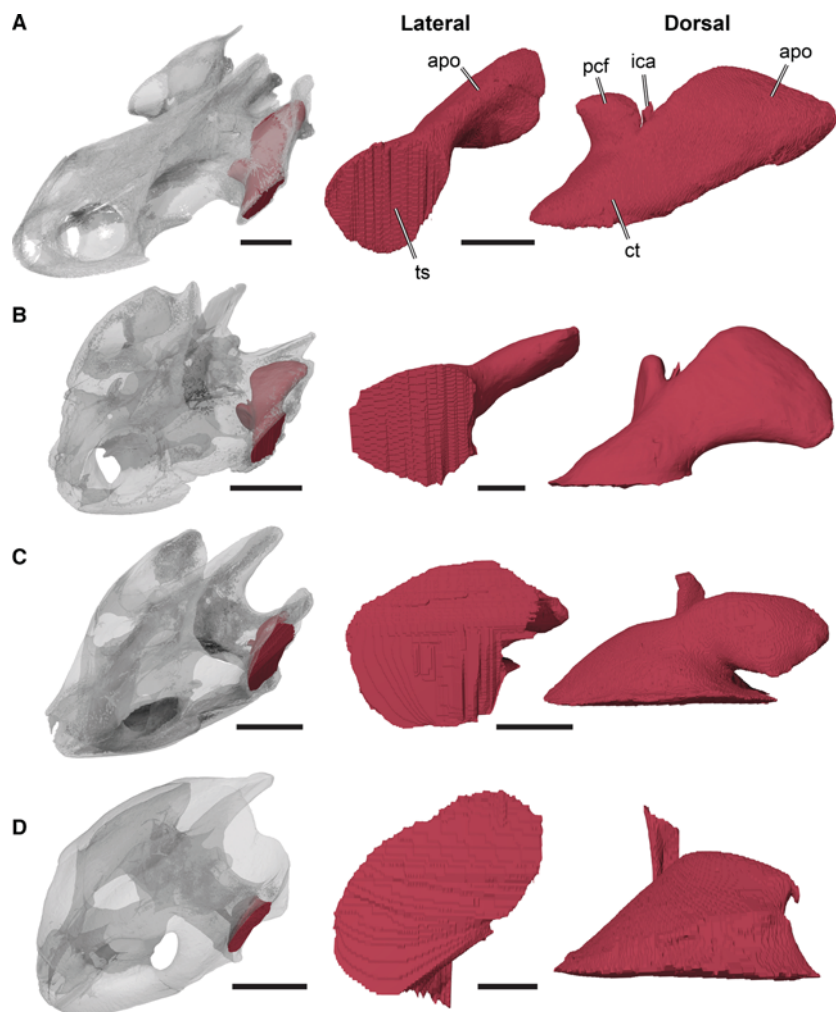


Fig. 2 Overview of shape variation of the middle ear cavity (cavum tympani and recesses) in selected extant turtles. (A) The chelid *Chelodina oblonga* (NHMUK 64.12.22). (B) The pelomedusoid *Pelomedusa subrufa* (SMF 70504). (C) The geoemydid *Batagur baska* (NHMUK 67.9.28.7), (D) The chelonioid *Chelonia mydas* (NHMUK 64.12.22). Left panel shows 3D renderings of transparent crania in left lateral and anterodorsal view with the lateral middle ear cavity rendered solid and in colour. The middle and right panels show close-ups of the middle ear cavity in various views. Scale bars: (A) 10 mm (cranium) and 5 mm (close-ups); (B) 10 mm (cranium) and 3 mm (close-ups); (C) 20 mm (cranium) and 10 mm (close-ups); (D) 50 mm (cranium) and 10 mm (close-ups). apo, antrum postoticum; ct, cavum tympani; ica, incisura columellae auris; pcf, precolumellar fossa; ts, tympanic surface.

underwater hearing; Hetherington, 2008), the relative size of the middle ear cavity (which could affect sound resonance and which has been reported to be low in chelonoids; Lenhardt et al. 1985; Hetherington, 2008) or the density of bone tissue encapsulating the ear (affecting sound transmission via bone-conduction, which has been reported to be low in chelonoids; Lenhardt et al. 1985). Although the tympanic-to-oval window area of sea turtles has been reported to be lower in the chelonoid *Chelonia mydas* (convergence ratio = 3; Lenhardt et al. 1985) in comparison with 'less aquatic turtles' (ratios > 8; Hetherington, 2008), most of the above observations so far remain anecdotal and proposed correlations with ecology have never been rigorously tested using comparative data.

To test a correlation of middle ear size and shape with ecology, we herein characterize the shape and volume of the middle ear cavity of a large sample of extant turtles for which habitat ecology is known, using 3D data, and perform a range of statistical analyses under consideration of the phylogenetic relationships of turtles that test whether habitat preferences correlate with the shape of the middle ear. We further quantify tympanic-to-oval window areas across our sample and therefore quantitatively address two previously proposed anatomical features that could be functionally linked to hearing in different habitats.

Materials and methods

Sampling and CT scanning

We assembled a dataset consisting of the high-resolution X-ray computed tomography (CT) scans of the skulls of 56 extant turtle species. These scans were collected from various facilities so that scanners and scanning parameters vary. All CT scans generated by us were deposited together with the scanning parameters at MorphoSource (<https://www.morphosource.org/>) under the Projects P462 (Evers & Benson, 2018) and P769 (Evers, 2019). Further scans were shared by Ingmar Werneburg and Irena Raselli (see Lautenschlager et al. 2018; Raselli, 2018), and one scan was downloaded from Digimorph (<http://digimorph.org/>) (see Supporting Information Appendix S1 and Table S1). Our sample was selected to represent all major clades of extant turtles and to maximize size variation (it includes skulls with lengths ranging from 16 mm in *Emydura subglobosa* to 219 mm in *Dermodochelys coriacea*), independent evolutionary transitions between habitat preferences (i.e. freshwater, marine and terrestrial), and locomotor modes as indicated by current phylogenies (Joyce et al. 2016; Pereira et al. 2017). The air-filled middle ear cavity and the temporal region of the skull were segmented using AMIRA 6.0.0 (Zuse Institute Berlin and FEI Visualization Sciences Group) and MIMICS 16.0 (Materialise HQ) and models were exported as surface models in.ply-format. The models were deposited at Dryad (<http://www.datadryad.org/>).

Morphometric measurements

The surface models of the temporal regions of the sampled skulls were used to make four different measurements by placing landmarks in three-dimensional space in AMIRA, and computing inter-

landmark distances or best-fit planes: (1) the inferred surface area of the tympanum, (2) the near-sagittal area of the fenestra ovalis, (3) the straight-line distance from the tympanum to the lateral margin of the incisura columellae auris, which corresponds to the mediolateral depth of the cavum tympani, and (4) measure 3 plus the straight-line distance from the columella auris to the fenestra ovalis (see below), which in total corresponds roughly with the length of the bony columella (Lenhardt et al. 1985). The area measurements were computed using a custom code (Supporting Information Appendix S2) in the program R (R Core Developmental Team) using landmarks placed around the perimeters of the tympanic recess and the fenestra ovalis. The distance measurements for the bony columella (measure 4) were calculated using the centroids of landmarks around the tympanic recess, the incisura columellae auris and the fenestra ovalis. Due to the inclusion of the incisura columellae auris, the measurements address the natural curvature of the columella. In addition, the volumes of the middle ear cavities were estimated in AMIRA using the surface models. Mean cross-sectional areas were estimated by dividing the volumes of the middle ear cavities by their mediolateral depths (measure 3). In addition, centroid sizes of the cavum tympani were taken from the analyses of spherical harmonics (see below) (Supporting Information Appendix S1 and Table S2).

Spherical harmonics

The surface models of the middle ear cavity were subjected to 3D spherical harmonic analyses to study shape variation using the software SPHARM v. 1.4 (<http://www.enallagma.com/SPHARM.php>) (Shen & Makedon, 2006; Shen et al. 2009). This method is an extension of elliptical Fourier analyses. It represents a 3D shape in terms of a sum of 3D sines and cosines on a sphere (Brechtbühler et al. 1995; Ritchie & Kemp, 1999) and captures details of curvature in more detail than geometric morphometrics (Shen & Makedon, 2006; Shen et al. 2009). This method has been applied to studying shape variation in the paranasal sinuses of carnivores (Curtis & Van Valkenburgh, 2014) and the reproductive organs of insects (McPeck et al. 2009, 2011), among others.

Before implementing the SPHARM analysis, all 3D models of the middle ear cavities were imported to MESHLAB v1.3.3 (Visual Computing Lab, ISTI, CNR), smoothed with 'Poisson Surface Reconstruction' (see 'Screened Poisson Surface Reconstruction' in later MESHLAB versions), using the default settings. This process distributes the vertices more equally to each other, minimizing irregularities of the surface texture, which can cause artefacts in the SPHARM analysis. Afterward, the models were simplified to 5000 triangular faces and 2502 vertices, and compared with the original models to assure that these modifications did not produce any artefacts. The final models were saved in MATLAB-format.

To align the middle ear cavities prior to SPHARM analysis, five landmarks were placed onto the models using the landmark function in AMIRA: (1) the most anterior point of the tympanum, (2) the most posterior point of the tympanum, (3) the most dorsal point of the tympanum, (4) the most ventral point of the tympanum and (5) the lateral opening of the columella auris, which is usually marked as an imprint on the surface model. The space defined by these five points is here referred to as the cavum tympani, as it broadly corresponds to this structure. The simplified models and landmark coordinates were also deposited at Dryad (<http://www.datadryad.org/>).

All model and landmark files were imported into SPHARM and superimposed using the measured centroid size to remove the effects of size and rotation (Zelditch et al. 2012). *Dermatemys*

mawii was chosen as the template taxon, as it was found to be closest to the consensus shape in a previous test run. The template taxon helps to align and register all other objects during the process. The spherical harmonic coefficients were finally computed to the 25th degree and spherical harmonic representations of each specimen were generated that retain as much detail as possible when compared with the original model. This value produces 2028 complex spherical harmonic coefficients for all three spatial dimensions in the final models. To ensure accuracy of this method, all models were afterwards compared with the original shapes.

Phylogeny

We used an updated version of the informal supertree of Foth & Joyce (2016) as the phylogenetic backbone for various statistical analyses, which differs from the published version in the position of some extinct marine turtles. In particular, pan-chelonoids were resolved according to Weems & Brown (2017) and protostegid turtles, including the 'dermochelyoids' of Bardet et al. (2013) and Lapparent de Broin et al. (2014), were placed as sister to thalassochelydians, as originally proposed by Joyce (2007) (but see Raselli, 2018 and Evers et al. 2019 for alternative phylogenetic placements for protostegids). The tree was time-calibrated in R using the package *paleotree* (Bapst, 2012) using information from the ages of fossils and from molecular clock studies. Select internal nodes were age-constrained based on dates obtained from molecular calibration studies (see Le & McCord, 2008; Vargas-Ramírez et al. 2008; Lourenço et al. 2012; Iverson et al., 2013; Joyce et al., 2013; Le et al. 2014; Spinks et al. 2016). The age of the root was adjusted with a time variable of 1 Ma. The remaining nodes were calibrated by extending zero-length branches to positive lengths by sharing time equally with rootward branches of non-zero length (Brusatte et al. 2008) using the 'equal' time-scaling method implemented in the *timePaleoPhy* function of the *PALEOTREE* package. Minimum branch length calibrations were not implemented to avoid the clustering of the divergence of Recent taxa, which lack molecular calibration ages, in the final time bin. Finally, the time-calibrated supertree was pruned to contain only taxa sampled in our dataset (Supporting Information Appendix S3).

Ecological categories

Turtles live in a broad set of habitats that range from fully aquatic (marine or freshwater) to fully terrestrial. As the full range of intermediates is apparent, it is difficult to rigorously categorize habitat preferences based on field observations (e.g. Joyce & Gauthier, 2004; Benson et al. 2011; Foth et al. 2017). However, Joyce & Gauthier (2004) could demonstrate that the forelimbs of turtles reflect the gradation from fully terrestrial to fully aquatic lifestyles. Therefore, we here discriminate five habitat preferences using the extent of the webbing of the forelimb as a proxy: (1) webbing absent, (2) webbing minor (i.e. webbing restricted to the most proximal portions of the digits), (3) webbing intermediate (i.e. webbing extends to the proximal ends of the ungual phalanges), (4) webbing extensive (i.e. webbing encloses the ungual phalanx of at least one digit), and (5) flippers present. The webbing-based grouping retrieved herein is not too different from habitat categorizations that use literature-based methods (e.g. Joyce & Gauthier, 2004), but the usage of an external morphological character as proxy was chosen objectively to evaluate turtles with intermediate habitat ecology.

These five categories were then regrouped in the following five variables, describing different degrees of lumping of forelimb webbing categories (Appendix S1, Table S2, Habitat grouping). Because they describe a continuum of variation, these were treated as ordered categorical variables (i.e. integers) rather than independent unordered categories.

Analyses of morphometric data

We tested the correlation of our morphometric measurements with our ecological (i.e. forelimb) categories, and with head size, which was estimated as the product of skull length, width and height (i.e. a box volume). To do this, we used phylogenetic generalized least square regression (pGLS; Grafen, 1989; Rohlf, 2001), which accounts for the non-independence of observations of species in a phylogeny by modifying the assumptions of ordinary least squares (OLS) regression analysis. All measurements were \log_{10} -transformed, and our analyses were conducted in R using functions from the packages *nlme 3.1-117* (Pinheiro et al. 2018) and *APE 3.2* (Paradis et al. 2004). pGLS yields identical results to OLS regression of phylogenetically independent contrasts, assuming Brownian motion (Felsenstein, 1985; see Garland & Ives, 2000), which is appropriate when a strong phylogenetic signal is present in the relationship between variables (i.e. the intercept of that relationship moves across the phylogeny). However, form-function relationships can be constrained by the physical laws of the universe, and therefore may lack phylogenetic signal (Motani & Schmitz, 2011). The strength of phylogenetic signal cannot be determined *a priori* but can be estimated during the fitting of pGLS regression models using the variable Pagel's lambda (Motani & Schmitz, 2011). Pagel's lambda describes scaling of a phylogeny between its full topology with branch lengths (lambda = 1; strong phylogenetic signal), and a 'star phylogeny', in which all tips diverge from the root of the tree, and are therefore treated as yielding statistically independent observations (Pagel, 1999; i.e. phylogenetic signal absent).

Because our morphometric measurements still contain information about size (see Table 1), we performed a phylogenetic size-correction against centroid size using pGLS with Brownian motion (Revell, 2009). This method estimates least-squares regression coefficients in the regression of size-dependent variables, while controlling for non-independence by including a phylogenetic backbone. The resulting size-corrected residuals were used for further statistical tests.

Analysis of spherical harmonic shape data

The representations of spherical harmonic analyses were applied to principal component analyses (PCA), which summarize major shape variation in a set of principal components (PCs). Using the broken-stick method (Jackson, 1993) in PAST 3.0.5 (Hammer et al. 2001) the first four principal components were found to be the most significant ones (see Appendix S1, Table S2). This stopping-rule method is based on randomly generated eigenvalues. If the sum of eigenvalues is divided randomly amongst the various components, the single eigenvalues will follow a broken-stick distribution. Here, observed shape variation is found to be meaningful if it is higher than the eigenvalues of the randomly generated broken-stick model.

In the next step, we tested how shape variation of the first each of the four PCs correlate with centroid sizes using pGLS (see above). As this method can only test for size correlation of single PCs, we

Table 1 Main results of the phylogenetic generalized least square (pGLS) regression analyses of middle ear measurements against head size (all log-transformed) and relevant ecological categories (overview of all regression results can be found in Appendix S1, Table S3).

Model rank	Model formula	R2	AICc weight	AICc	Lambda	Variable	Slope	P-value
Tympanum surface area (CT_area)								
1	CT_area ~ log10(head_size)	0.85	0.54	-34.21	0.6	Intercept	-1.157	< 0.001
						log10(head_size)	0.669	< 0.001
2	CT_area ~ log10(head_size) + forelimb 4	0.85	0.116	-31.13	0.69	Intercept	-1.146	< 0.001
						log10(head_size)	0.643	< 0.001
						forelimb 4	0.083	0.056
3	CT_area ~ log10(head_size) + forelimb 3	0.85	0.102	-30.87	0.69	Intercept	-1.11	< 0.001
						log10(head_size)	0.635	< 0.001
						Forelimb 3	0.073	0.057
4	CT_area ~ log10(head_size) + forelimb 5	0.84	0.09	-30.62	0.65	Intercept	-1.184	< 0.001
						log10(head_size)	0.657	< 0.001
						Forelimb 5	0.091	0.112
Fenestra ovalis area (FO_area)								
1	FO_area ~ log10(head_size)	0.83	0.823	-54.51	0.23	Intercept	-1.337	< 0.001
						log10(head_size)	0.469	< 0.001
Cavum tympani chamber centroid size (chamber size)								
1	Chamber_size ~ log10(head_size)	0.91	0.931	-155.65	0.85	Intercept	1.134	< 0.001
						log10(head_size)	0.295	< 0.001
Middle ear volume (chamber volume)								
1	Chamber_volume ~ log10(head_size) + forelimb 1	0.93	0.57	-52.25	-0.1	Intercept	-1.205	< 0.001
						log10(head_size)	0.867	< 0.001
						Forelimb 1	-0.044	0.001
2	Chamber_volume ~ log10(head_size)	0.93	0.262	-50.69	0.34	Intercept	-1.154	< 0.001
						log10(head_size)	0.837	< 0.001
3	Chamber_volume ~ log10(head_size) + forelimb 2	0.93	0.097	-48.71	-0.07	Intercept	-1.104	< 0.001
						log10(head_size)	0.845	< 0.001
						Forelimb 2	-0.038	0.021
Distance from tympanum to fenestra ovalis via columella auris (distCT_FO)								
1	DistCT_FO ~ log10(head_size)	0.93	0.855	-138.04	0.7	Intercept	-0.626	< 0.001
						log10(head_size)	0.376	< 0.001
Ratio of tympanum area to fenestra ovalis area (CT_area/FO_area)								
1	CT_area/FO_area ~ log10(head_size)	0.3	0.458	-31.25	0.44	Intercept	0.21	0.195
						log10(head_size)	0.194	< 0.001
2	CT_area/FO_area ~ log10(head_size) + forelimb 3	0.3	0.17	-29.27	0.33	Intercept	0.278	0.075
						log10(head_size)	0.154	< 0.001
						Forelimb 3	0.079	0.021
3	CT_area/FO_area ~ log10(head_size) + forelimb 4	0.29	0.1	-28.21	0.33	Intercept	0.217	0.156
						log10(head_size)	0.169	< 0.001
						Forelimb 4	0.079	0.046
4	CT_area/FO_area ~ log10(head_size) + forelimb 1	0.29	0.099	-28.19	0.37	Intercept	0.219	0.154
						log10(head_size)	0.164	< 0.001
						Forelimb 1	0.054	0.03
5	CT_area/FO_area ~ log10(head_size) + forelimb 5	0.28	0.063	-27.28	0.42	Intercept	0.182	0.253
						log10(head_size)	0.184	< 0.001

(continued)

Table 1 (continued)

Model rank	Model formula	R2	AICc weight	AICc	Lambda	Variable	Slope	P-value
6	CT_area/FO_area ~ log10 (head_size) + forelimb 2	0.28	0.062	-27.25	0.37	Forelimb 5	0.083	0.139
						Intercept	0.18	0.245
						log10(head_size)	0.175	< 0.001
						Forelimb 2	0.052	0.056
Cavum tympani chamber width (chamber_width)								
1	Chamber_width ~ log10 (head_size)	0.9	0.909	-120.49	0.26	Intercept	-0.846	< 0.001
						log10(head_size)	0.353	< 0.001
Middle ear volume, mean cross-sectional area (chamber_cross-section)								
1	Chamber_cross- section ~ log10(head_size)	0.85	0.83	-64.78	0.77	Intercept	-0.344	0.012
						log10(head_size)	0.489	< 0.001

additionally applied a method that evaluates linear models for high-dimensional data in a phylogenetic context (hereafter: D.pGLS) (Adams, 2014). Using the statistical equivalency between parametric methods using covariance matrices and methods based on distance matrices (Adams, 2014), all four PCs can be analysed in a single multivariate block against log₁₀-transformed centroid size. The method is implemented in the R package *geomorph* (Adams & Otárola-Castillo, 2013) and performs analysis of variance (ANOVA) and regression models in a phylogenetic context under a Brownian motion model of evolution and uses permutation procedures to assess statistical hypotheses.

In addition, we tested whether the PCA data of the SPHARM analysis are influenced by the phylogenetic relationship of turtles using *K* statistics (Blomberg et al. 2003) and Pagel's lambda (Pagel, 1997), which is implemented in R package *phytools* (Revell, 2012).

Finally, we tested for statistical overlap of different ecological groupings (see above) based on the size-corrected residuals of morphometric measurements and PCA data generated from the SPHARM analysis using D.pGLS (see above). As the grouping of habitat preferences could be biased by the phylogenetic relationship of turtles, we additionally applied phylogenetic flexible discriminant analyses (pFDA) (see Motani & Schmitz, 2011; Schmitz & Motani, 2011), which removes the phylogenetic bias from the categorical variable. This extension of classical discriminant analyses first estimates Pagel's lambda to test how the grouping correlates with phylogeny, and then uses this assessment to control for phylogenetic non-independence during the actual discriminant analyses.

Institutional abbreviations

AMNH, American Museum of Natural History, New York, NY, USA; BP, Bernard Price Institute, University of the Witwatersrand, Johannesburg, South Africa; FMNH, Field Museum of Natural History, Chicago, IL, USA; IW, Research Collection of Ingmar Werneburg, University of Tübingen, Tübingen, Germany; MPEF, Museo Paleontológico Egidio Feruglio, Trelew, Argentina; NHMUK, Natural History Museum, London, UK; NHMW, Naturhistorisches Museum Wien, Vienna, Austria; NMB, Naturhistorisches Museum Basel, Basel, Switzerland; NMS, National Museums Scotland, Edinburgh, UK; PIMUZ, Paläontologisches Institut und Museum der Universität Zürich, Zurich, Switzerland; SMF, Naturmuseum Senckenberg, Frankfurt, Germany; SMNS, Staatliches Museum für Naturkunde

Stuttgart, Stuttgart, Germany; TMM Texas Memorial Museum, Austin, TX, USA.

Results

Morphometric measurements

All measurements scale positively with head size (Table 1; Figs 3 and 4). In fact, for most middle ear measurements, head size is the only of our variables that provides a statistically significant explanation. This is true of fenestra ovalis area, cavum tympani chamber centroid size, distance from cavum tympani to fenestra ovalis (via columella auris), cavum tympani chamber width, and a cross-sectional area of the middle ear cavity. For all of these variables, adding any of our forelimb traits to the model results in negligible Akaike information criterion (AICc) weights, rejecting the likelihood of a relationship with habitat ecology (Table 1, Supporting Information Appendix S1 and Table S3).

For a second set of middle ear variables, we find that forelimb traits are included alongside head size in the set of non-negligible regression models, but that these models are worse than those including only head size. This is true for the tympanum surface area and the ratio of the tympanum surface area to the fenestra ovalis area (i.e. our proxy of the acoustic transformer ratio; Appendix S1, Table S2). The slopes of our forelimb variables in these models are non-significant [$P = 0.056$ (forelimb 4 for cavum tympani surface area)] or significant [$P = 0.021$ (forelimb 3 for ratio of cavum tympani surface area to fenestra ovalis area)]. The signs of the slopes suggest that turtles that spend more time in water have a proportionally larger tympana. However, because these models do not receive the top AICc weights, they should be interpreted as being only weakly supported.

The only middle ear measurement that shows a strong relationship with our forelimb traits is the volume of the middle ear cavity. For this measurement, the best model

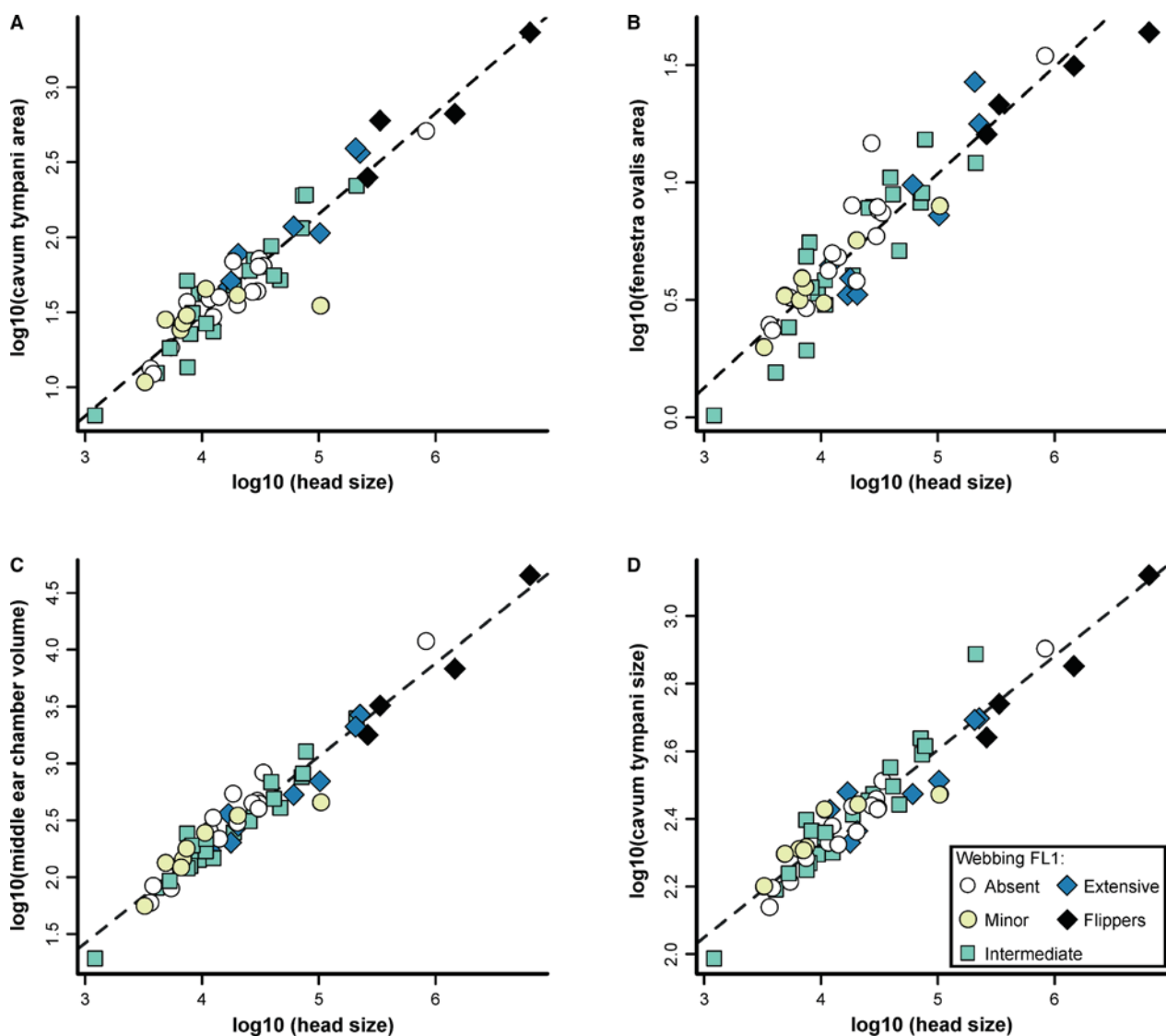


Fig. 3 Results of the phylogenetic generalized least square (pGLS) regression analyses of different log₁₀-transformed morphometric measurements from the middle ear against the head size (box volume) under consideration of ecological categories (Forelimb1, FL1). (A) Inferred surface area of the tympanum. (B) Near-sagittal area of the fenestra ovalis. (C) Volumes of the lateral middle ear cavity (LMEC). (D) Centroid sizes of the cavum tympanum.

according to AICc weights includes both head size and forelimb 1 as explanatory variables. Forelimb 1 has a strongly significant ($P = 0.01$) negative slope, indicating that more aquatic turtles have volumetrically smaller middle ear cavities. The slope of forelimb 1 (slope = -0.044), taken over the range of the hands 1 variable (1–5), implies that the most aquatic turtles in our sample have middle ear cavities with two-thirds (0.667) the volume of terrestrial turtles. Nevertheless, it is clear that there is substantial overlap in relative chamber volume between habitat groups (Figs 3 and 4). Furthermore, a model explaining the volume of the middle ear cavity using only head size has non-negligible AICc weight, just slightly less than half that of the best model. Our results therefore provide only tentative support

for a relationship between the volume of the middle ear cavity and habitat preferences in turtles that may warrant further investigation.

The slope of head size in explanatory models indicates approximate isometry for the tympanum surface area (slope = 0.669, compared with 0.667 for isometry), strong negative allometry for fenestra ovalis area (slope = 0.496; compared with 0.666 for isometry), weak negative allometry for cavum tympani centroid size (slope = 0.295; compared with 0.333 for isometry), weak positive allometry for the distance from the centroid of the tympanum to that of the fenestra ovalis (slope = 0.371 compared with 0.333 for isometry), near-isometry for the distance between the tympanum and columella auris (=width of the cavum tympani;

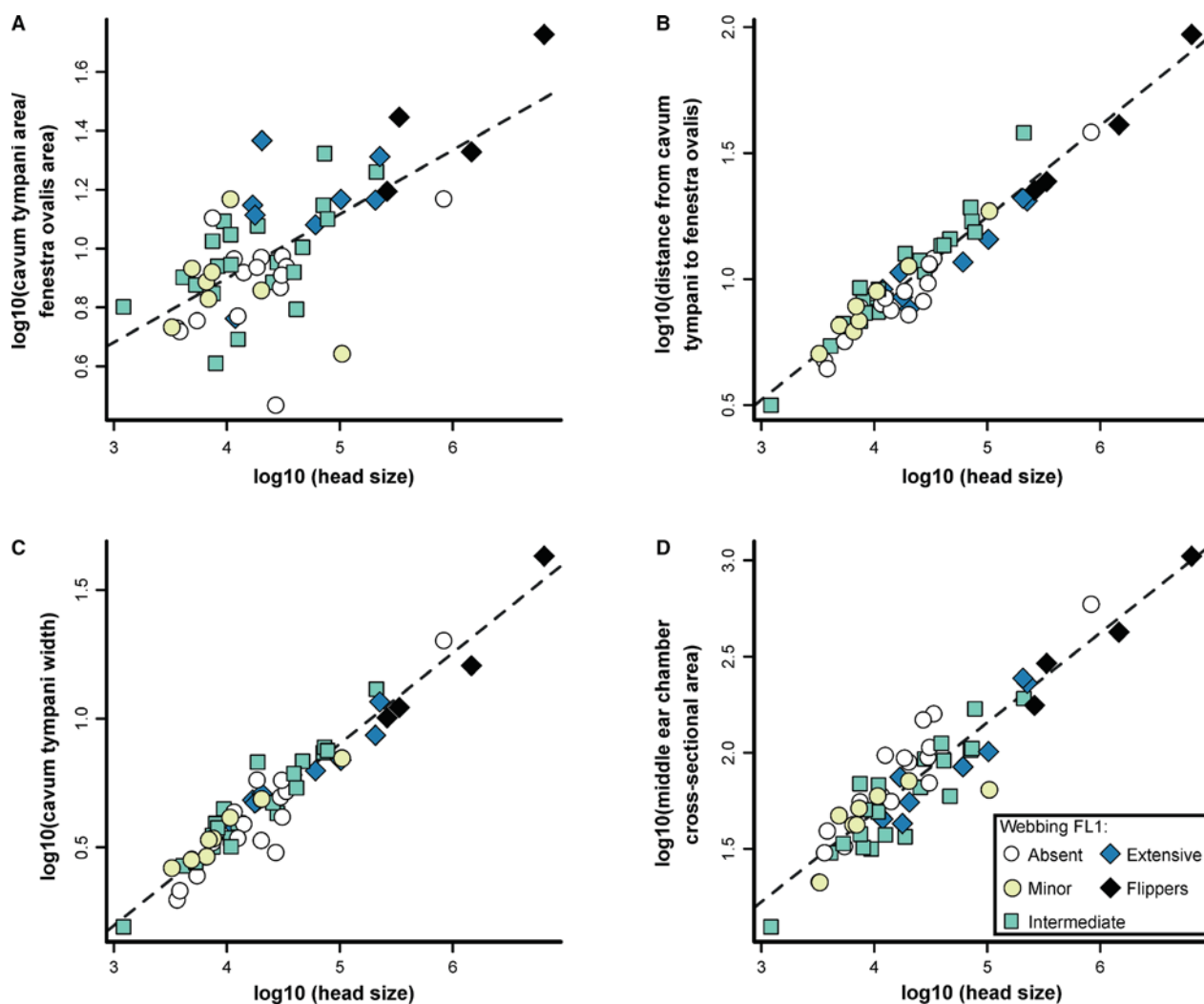


Fig. 4 Further results of the phylogenetic generalized least square (pGLS) regression analyses of different log₁₀-transformed morphometric measurements from the middle ear against the head size (box volume) under consideration of ecological categories (Forelimb1, FL1). (A) Ratio between surface area of the tympanum and sagittal area of the fenestra ovalis. (B) Distance from the tympanum to the fenestra ovalis. (C) Distance from the tympanum to the lateral margin of the incisura columellae auris. (D) Mean cross-sectional areas.

slope = 0.352, compared with 0.333 for isometry), and negative allometry for the mean cross-sectional area of the middle ear cavity (slope = 0.489, compared with 0.666 for isometry). The only taxon that lies significantly outside the found correlations is *Platysternon megacephalum*, which has a disproportionately small middle ear cavity compared with its head size.

PCA of spherical harmonics

The first four principal components were found to explain 76.6% of total shape variation (PC1: 39.5%; PC2: 17.6%; PC3: 10.9% and PC4: 8.6%). All subsequent principal components each describe less than 5% of variation (Supporting Information Appendix S1 and Table S4). Negative values of PC1 are associated with a middle ear cavity that is

horizontally oriented and that has a long and dorsoventrally flattened antrum postoticum, which is medially inclined with respect to the cavum tympani. The cavum tympani tends to be relatively small and the tympanum is oval in shape, and anteroposteriorly longer than dorsoventrally tall. In contrast, positive PC1 values describe a middle ear cavity that is slightly inclined dorsoventrally and an enlarged cavum tympani that is aligned mediolaterally and associated with a short and deep antrum postoticum. The tympanum is oval in shape, and dorsoventrally taller than anteroposteriorly long (Fig. 5, Supporting Information Appendix S4).

Negative values of PC2 capture middle ear cavities that are slightly shorter and mediolaterally thicker. The antrum postoticum is relatively strongly medially directed and the cavum tympani is ventrally expanded. In

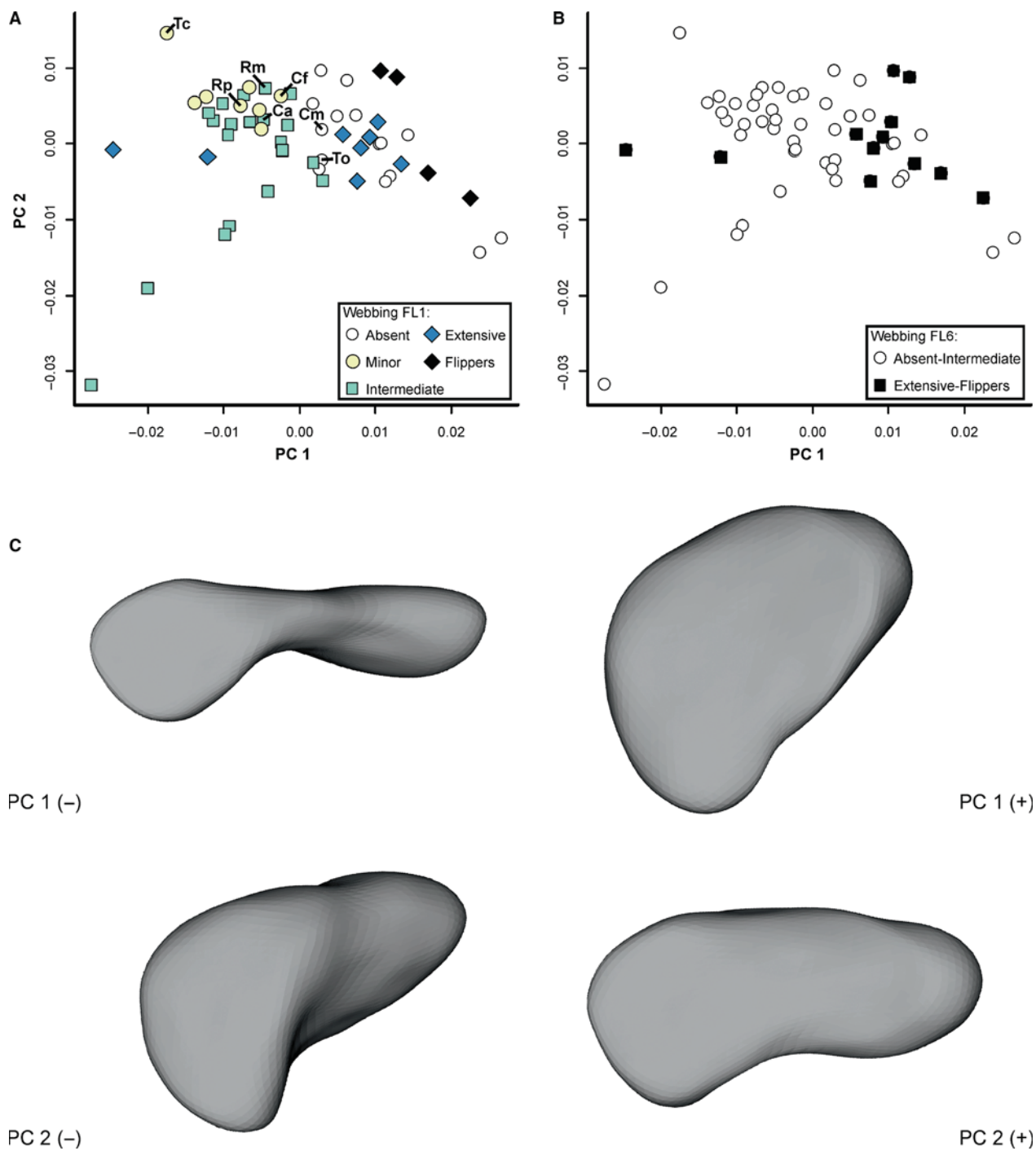


Fig. 5 Results of the principal component analyses and 3D spherical harmonic analyses. (A) Morphospace of the lateral middle ear cavity of turtles for PC1 and PC2 showing the distribution of ecological categories according to Forelimb1 (FL1). (B) Same plot showing the distribution of ecological categories according to Forelimb6 (FL6). (C) Major shape variation of the lateral middle ear cavity for PC1 and PC2 in lateral view. Ca, *Cuora amboinensis*; Cf, *Cuora flavomarginata*; Cm, *Cuora mouhotii*; Rm, *Rhinoclemmys melanosterna*; Rp, *Rhinoclemmys pulcherrima*; Tc, *Terrapene coahuila*; To, *Terrapene ornata*.

contrast, positive PC2 values are associated with elongated and narrow middle ear cavities, in which the antrum postoticum extends posteriorly from the cavum tympani (Fig. 5, Appendix S4).

Negative values of PC3 describe anteroposteriorly elongate middle ear cavities, in which the cavum tympani is short and ventrally expanded with respect to the antrum postoticum, while the antrum postoticum itself is

dorsoventrally flattened and anteroposteriorly elongated and shows a bulbous posterior end. In contrast, positive PC3 values capture short middle ear cavities with an anteroposterior elongated cavum tympani and a short and deep antrum postoticum with a pointed posterior tip. The ventral margin of the antrum postoticum is continuous with the cavum tympani (Fig. 6, Appendix S4).

Negative values of PC4 are associated with a narrow and elongate middle ear cavity, which is inclined along the anterior-posterior axis. The area of the tympanum is slightly enlarged and continuous with the ventral margin of the antrum postoticum. The latter is elongated and pointed posteriorly. In contrast, positive PC4 values describe broadened middle ear cavities that are oriented along the anterior-posterior axis. The area of the tympanum is slightly decreased, and the antrum postoticum is shortened and has a bulbous posterior end (Fig. 6, Appendix S4).

Both regression tests (pGLS for each PC and D.pGLS for all PCs) indicate that the first four PCs are not correlated with \log_{10} -transformed centroid size, meaning that size does not predict the shape of the middle ear cavity. In addition, K statistics and Pagel's lambda reveal that the cavity shape correlates with the phylogenetic relationship of turtles on a significant level ($K = 0.5625$, $P = 0.001$; $\lambda = 0.8719$, $P = < 0.0001$).

Correlation with habitat

Based on pFDA, the total rate of misidentifications for the size-corrected residuals of the morphometric measurements ranges between 0.14 (two categories) and 0.46 (four categories). Using the original categories of habitat preferences based on the degree of webbing and all morphometric measurements, turtles without webbing (category 1 = terrestrial turtles) were correctly identified in 9 of 15 cases. In contrast, no turtle was correctly predicted to have minor forelimb webbing (category 2). Turtles with intermediate webbing (category 3) were correctly identified in 16 of 21 cases, whereas the discrimination of turtles with extensive webbing (category 4) was successful in 5 of 8 cases. Finally, turtles with flippers (category 5) were correctly identified in 2 of 4 cases (Fig. 7A; Supporting Information Appendix S1 and Table S5). Combining different categories with each other does not improve the rate of correct identifications substantially until only two categories are left (i.e. aquatic and terrestrial). A comparison between aquatic and terrestrial turtles following the scheme 'forelimb5' (category 1 + 2 vs. category 3 + 4+5) found aquatic turtles to be correctly identified in 32 of 33 cases, whereas 8 of 23 turtles were found to be terrestrial. By applying the scheme 'forelimb6' (category 1 + 2 + 3 vs. category 4 + 5) aquatic turtles were correctly identified in 9 of 12 cases, whereas 39 of 44 turtles were found to have stronger terrestrial affinities (Appendix S1 and Table S5).

Using D.pGLS, the original habitat preferences cannot be discriminated from each other based on morphometric measurements. Only for the schemes 'forelimb3' and 'forelimb6' was a differentiation between the different categories possible (Supporting Information Appendix S1 and Table S6).

The PCA results from SPHARM analysis reveal better discrimination of the different habitat groups than using measurements. The total rate of misidentifications ranges from 0.09 (two categories) to 0.34 (four categories). Turtles lacking webbing in the forelimbs (category 1 = terrestrial turtles) were correctly identified in 11 of 15 cases, whereas 1 of 8 turtles with minor webbing (category 2) were correctly tagged. Turtles with intermediate webbing (category 3) were successfully identified in 18 of 21 cases, and the discrimination of turtles with extensive webbing (category 4) was correct in 6 of 8 cases. Finally, turtles with flippers (category 5) were correctly identified in 3 of 4 cases. When compared with the previous results of pFDA, information of shape led to a slightly better discrimination (Fig. 7B–D; Appendix S1, Table S5). As for morphometric measurements, combining different categories with each other does not improve the results, except for the comparison between aquatic and terrestrial turtles. Following the scheme 'forelimb5', aquatic turtles were correctly identified in 32 of 33 cases, whereas 10 of 23 turtles were found to be terrestrial. Using the scheme 'forelimb6', 41 of 44 were found to show terrestrial affinities, and 10 of 12 cases were identified as fully aquatic (Appendix S1, Table S5).

As in the former case, D.pGLS cannot discriminate between the original habitat preferences when PCA data are used. Only for the scheme 'forelimb6' was a differentiation between the different categories possible (Appendix S1, Table S6).

Although different habitat groups can be discriminated to some extent, the morphospace generally indicates a weak correlation between shape and ecology, as the position of the different habitat groups within the morphospace does not reflect the gradient from terrestrial to marine, which is expressed by the degree of webbing. In contrast, turtles without webbing plot closely together with those having flippers, whereas turtles with small webbing are partly isolated but overlap marginally with those having intermediate or extensive webbing. Finally, turtles with extensive webbing overlap intensively with those having no or intermediate webbing.

Discussion

The evolutionary history of extant turtles is characterized by shifts in habitat preferences from terrestrial to freshwater (e.g. Testudines, i.e. crown-group turtles), freshwater to terrestrial (e.g. Testudinidae, i.e. tortoises), and freshwater to marine (e.g. Chelonioidae, i.e. sea turtles). As turtles with different habitat preferences show morphological

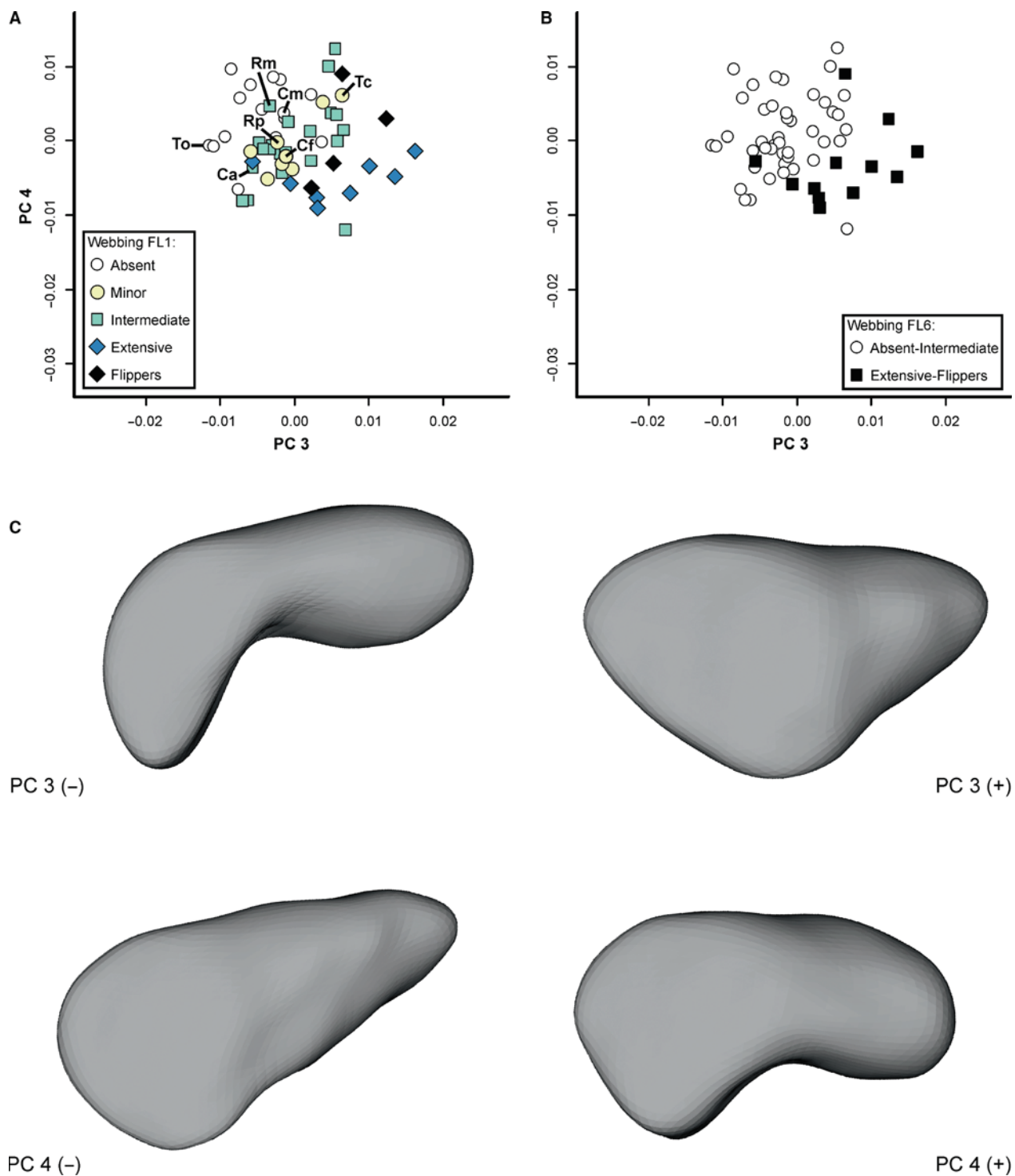


Fig. 6 Results of the principal component analyses and 3D spherical harmonic analyses. (A) Morphospace of the lateral middle ear cavity of turtles for PC3 and PC4 showing the distribution of ecological categories according to Forelimb1 (FL1). (B) Same plot showing the distribution of ecological categories according to Forelimb6 (FL6). (C) Major shape variation of the lateral middle ear cavity for PC3 and PC4 in lateral view. *Ca*, *Cuora amboinensis*; *Cf*, *Cuora flavomarginata*; *Cm*, *Cuora mouhotii*; *Rm*, *Rhinoclemmys melanosterna*; *Rp*, *Rhinoclemmys pulcherrima*; *Tc*, *Terrapene coahuila*; *To*, *Terrapene ornata*.

differences in the skull (Foth et al. 2017), shell (Claude et al. 2003; Domokos & Várkonyi, 2008; Benson et al. 2011; Polly et al. 2016) and forelimbs (Joyce & Gauthier, 2004; Renous

et al. 2008), differences have been interpreted to reflect these ecologies. As the physical demands of hearing are vastly different for animals in water vs. in air, modifications

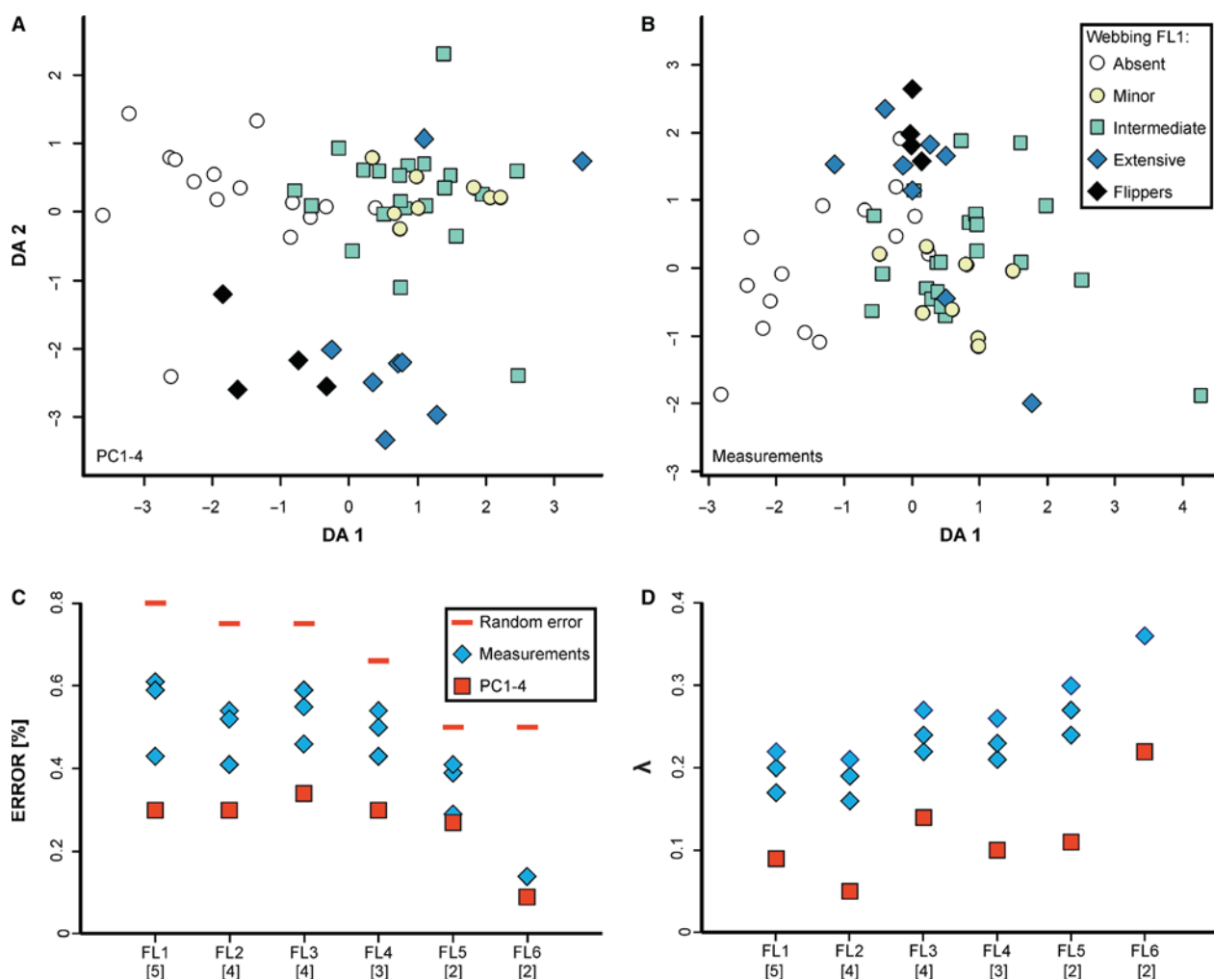


Fig. 7 Results of the phylogenetic flexible discriminant analyses (pFDA) testing ecological constraints for the middle ear of turtles. (A) pFDA plot showing the division of ecological categories according to Forelimb1 (FL1) using the first four PCs from the SPHARM analyses. (B) pFDA plot showing the division of ecological categories according to Forelimb1 (FL1) using morphological measurements. (C) Percentage error for correct identification of different combinations of ecological categories (Forelimb1 to Forelimb6) in the pFDA based on morphological measurements and PCA data. (D) Pagel's lambda showing the strength of phylogenetic signal for the different combinations of ecological categories in the pFDA based on morphological measurements and PCA data.

can be expected in the auditory system of turtles as well. However, little is known about the hearing physiology of turtles, making conclusions on how their middle ear morphology is related to habitat preferences and hearing performance difficult. Some case studies indicate that the frequency spectrum of hearing in turtles is generally similar in air and under water (e.g. Christensen-Dalsgaard et al. 2012; Zeyl & Johnston, 2015; Piniak et al. 2016, see also Lavender et al. 2014). Extremely little is also known about the function of hearing in turtles. Several studies have documented vocalizations in turtles (see Colafrancesco & Gridi-Papp, 2016 for a recent summary) that can reasonably be interpreted as calls utilized in communication, though experimental setups are still too preliminary to demonstrate their function with confidence. Additional functions of

hearing are both possible and probable (i.e. general environmental awareness, prey capture, predator avoidance), but their contribution has also yet to be demonstrated.

We investigated the relationship of habitat (aquatic/terrestrial) to various measures of middle ear chamber size and shape, and inferred functional indices such as tympanum size and acoustic transformer ratio. We were surprised to find that many of these measures do not differ in a significant and co-ordinated way between aquatic and terrestrial turtles. In particular, the acoustic transformer ratio has been suggested to be higher in terrestrial turtles compared with aquatic species (Hetherington, 2008) and this is expected under classic models of impedance-matching hearing in tetrapods (Nummela & Thewissen, 2008). However, we found no evidence of this relationship in turtles. Our results

regarding middle ear cavity volume and shape are explained in more detail below.

Middle ear cavity volume

Our dataset indicates that the volume of the middle ear cavity of turtles (i.e. the combined volume of the cavum tympani, antrum postoticum and precolumellar fossa) scales with a negative allometry with respect to head size (Table 1). This broadly supports the conclusion of Willis et al. (2013); $n = 25$ species), though with a larger dataset ($n = 56$ species). However, whereas Willis et al. (2013) did not find any statistical differences between the relative middle ear volume of marine and non-marine turtles, our study indicates that more aquatic turtles (i.e. turtles with better developed webbing) tend to have proportionally smaller middle ear cavities than terrestrial ones. In fact, fully terrestrial turtles (i.e. turtles that lack webbing), such as testudinids, have cavity volumes that are about 33% larger than those of fully aquatic turtles, such as trionychians and chelonoids. We also find weak statistical evidence that more aquatic turtles have a proportionally larger tympanic surface area, but correlations between habitat categories (based on our forelimb proxy) and other measurements of the middle ear are otherwise absent.

The occupation of air volume within the middle ear cavity is reduced minimally by the presence of the columella, extracolumella, ligaments, tissues that line the cavity, and the tympanum itself, as documented by cross-sections of the middle ear cavity of the freshwater aquatic turtle *Trachemys scripta* (Hetherington, 2008). However, a substantial amount of the potential air volume can also be occupied by fatty tissues, at least in chelonoids (sea turtles), as demonstrated by studies of *Caretta caretta* and *Chelonia mydas* (e.g. Ridgway et al. 1969; Lenhardt et al. 1985). It is therefore important to note that the size of the middle ear cavity as measured herein can only serve as a maximum estimate for the actual volume of gases held in this space and that possible soft-tissue specializations may be masked by our study design. This requires further investigation. Nevertheless, the reduced relative size of the osteological size of the middle ear cavity in more aquatic turtles, documented by our study, is consistent with the further reduction of air volume in this chamber caused by the presence of fatty tissues in the most strongly aquatic turtles (sea turtles).

The volume of the middle ear cavity is known to influence the performance of the ear because its size affects stiffness of the auditory chain and its behaviour as a resonance chamber in air or in water (Christensen-Dalsgaard et al. 2012; Mason, 2016). In many groups of terrestrial amniotes, particularly mammals, the middle ear cavity can be greatly inflated as a way to aid in the specialized hearing of low-frequency sounds (e.g. Legouix & Wisner, 1955; Webster & Webster, 1975; Rosowski & Graybeal, 1991; Rosowski, 1992; Coleman & Colbert, 2010; Mason, 2016),

but variation in middle ear volume within closely related groups of mammals far exceeds that found in our entire sample of turtles, especially relative to body size. The middle ear of turtles is therefore notable for lacking extreme specializations in regard to its volume.

A minor degree of specialization is nevertheless apparent, as terrestrial turtles have slightly larger middle ear cavities than fully aquatic turtles of similar size. This correlation may further be amplified in living turtles, as the size of the air-filled middle ear cavity of marine turtles is further reduced by the presence of fatty tissues (e.g. Ridgway et al. 1969; Lenhardt et al. 1985). Future work will need to clarify if the relatively minor difference in chamber volume between aquatic and terrestrial is caused by differing acoustic demands upon their hearing in air or under water. As an alternative, it is possible that the size of the air-filled chamber is minimized in aquatic turtles to aid diving, as the air-filled portion of the middle ear, together with the surrounding tissues, is subjected to strong compressive forces under water. Along those lines, Lenhardt et al. (1985) already hypothesized that the fat layer found in marine turtles may allow the middle ear of these animals more easily to expel air through the Eustachian tube when diving (Lenhardt et al. 1985).

Middle ear cavity shape

Our study confirms that a great amount of shape variation is present in the middle ear cavity of turtles (Figs 5 and 6), particularly in regard to the size and shape of the antrum postoticum. However, we find no correlation of shape with size or with habitat preferences. This can be exemplified by sampled genera that include species with different habitat adaptations. Three *Cuora* species (*Cuora mouhotii*: webbing-0; *Cuora flavomarginata*: webbing-1; *Cuora amboinensis*: webbing-2) and two *Rhinoclemmys* species (*Rhinoclemmys pulcherrima*: webbing-1; *Rhinoclemmys melanosterna*: webbing-2) cluster closely together in the PCA morphospace, despite difference in ecology. Only the two *Terrapene* species (*Terrapene ornata*: webbing-0; *Terrapene coahuila*: webbing-1) show strong differences in middle ear shape (Figs 5A and 6A), differing in the anteroposterior extent of the antrum postoticum and the dorsoventral extent of the surface area of the tympanum. In light of the general lack of an ecological signal in our data, it is, however, highly speculative whether this divergence is the result of actual habitat adaptations. Therefore, we highlight three other factors that may plausibly control the shape of the middle ear cavity: diving performance, hearing specializations, and the shape of surrounding cranial structures.

Our analyses demonstrate that the antrum postoticum of extant marine turtles is strongly reduced in size, in contrast to nearly all other turtles, which possess clearly developed antra postotica and/or precolumellar fossae. As our taxon sample includes only one monophyletic group of marine

turtles, Cheloniodea, it remains speculative whether this observation can truly be attributed to a marine lifestyle. The reduced antrum postoticum might merely be an apomorphy of chelonioids, unrelated to acoustic function, or it may be an adaptation to their marine lifestyle. It is nevertheless plausible, for instance, that a more spherical middle ear cavity (i.e. a middle ear cavity that lacks an antrum postoticum) resists water pressure better during diving than a middle ear cavity associated with elongate diverticulae. Fossils provide evidence of extinct groups that became adapted to marine life independently of the extant clade of sea turtles (chelonioids) (e.g. bothremydids, sandownids, thalassochelydians; see Evers & Benson, 2019 for a review). Fossils of these extinct marine turtles may clarify this question. Indeed, we note that the antrum postoticum is also reduced in marine-adapted bothremydids and sandownids (Gaffney et al. 2006; Tong & Meylan, 2013). A similar reduction of the antrum postoticum is also apparent for the extant freshwater aquatic *Carettochelys insculpta*, which has limbs that take the form of well-developed flippers. However, for now, we are unaware of data that would suggest that *C. insculpta* dives deeper than its closest relatives, trionychids, which have well-developed antra postotica. Additionally, some extinct marine Jurassic thalassochelydians, such as *Solnhofia parsoni* or *Plesiochelys planiceps*, also have well-developed antra postotica that extend deeply into the squamosals (e.g. Gaffney, 1975, 1976; Anquetin et al. 2017; Evers & Benson, 2019).

The enlarged middle ear cavity of many mammals is characterized by the presence of well-developed internal walls that create subdivisions. These sub-cavities act in unison at low frequencies but are decoupled from one another at high frequencies, allowing the animal to hear optimally at a greater range of frequencies (Mason, 2016). As the antrum postoticum and precolumellar fossa of some turtles are notably separate from the tympanic cavity, it is possible that this morphology may also improve hearing across a broader spectrum. It is far outside the reach of this study to compile comparative hearing data of a broad set of extant turtles to test this hypothesis. However, as the diverticulae are so small relative to the main cavity, in contrast to the enormous sub-chambers found in mammals, we are sceptical that their presence will be shown to have a significant impact on hearing.

The middle ear cavity of turtles is typically formed by the quadrate and squamosal (Gaffney, 1979). The quadrate furthermore forms the medial portions of the middle ear, helps brace the chondrocranium against the dermatocranium, and articulates with the mandible (Gaffney, 1979) and the squamosal serves as the attachment site for numerous muscles pertaining to jaw closure and neck movement (Werneburg, 2011, 2013, 2015; Jones et al. 2012; Ferreira & Werneburg, 2019). It is therefore not surprising that these bones, in particular the squamosal, show an enormous amount of shape diversity across the phylogeny of turtles

(Werneburg, 2011, 2013, 2015; Foth & Joyce, 2016). As the function of the air-filled portion of the middle ear is mostly determined by its size, not its shape (Mason, 2016), we hypothesize that its shape may at least in part be controlled by factors fully unrelated to hearing, such as jaw closure, neck retraction or shape of the temporal region. A preliminary two-block partial least squares regression analysis (Rohlf & Corti, 2000) finds a significant correlation for principal components from the SPHARM analysis and skull box (i.e. size-corrected log-transformed height, length and width measurements), which do not persist if the data is corrected for phylogeny (Adams & Felice, 2014). The morphometric measurements are uncorrelated with skull box measurements in both types of analysis (see Supporting Information Appendix S5). This lack of correlation only indicates that there is no strong relationship of middle ear cavity shape to 'global' skull morphology, it does not rule out constraints of shape that are imposed by the specific morphology of the temporal region. This has to be tested in a more sensitive shape analysis in a future approach.

The evolutionary history of the turtle ear

Although the origin of hearing in amniotes has been the subject of much interest over the course of the last decades, only little attention has been accorded to the origin of hearing in turtles (e.g. Willis et al. 2013; Sobral et al. 2016). We therefore here highlight the available paleontological evidence and discuss the adaptive significance of hearing in turtles.

In the oldest known turtle (i.e. amniote covered with a full shell) with preserved cranial remains, the Late Triassic *Proganochelys quenstedtii*, the quadrate and squamosal jointly form a moderate depression along the side of the skull, and this depression was likely covered by a tympanum which housed an air-filled middle ear cavity (Gaffney, 1990; Sobral et al. 2016; pers. obs. SMNS 16980). The columella of this turtle, however, is a solid, slightly recurved bar that articulates with the quadrate and not the tympanum. It is therefore apparent that this turtle lacked an impedance-matching ear and that the impedance-matching ability of turtles evolved independently from other amniotes (Sobral et al. 2016). Furthermore, because the middle ear is not enclosed by bone in *P. quenstedtii* (i.e. neither the cavum acustico-jugulare nor the cavum tympani are formed), osteological correlates that would demonstrate the precise morphology of the middle ear are lacking. Nevertheless, most authors presume that the pericapsular recess was absent in *P. quenstedtii* (Clack & Allin, 2004). A series of Early to Middle Jurassic turtles, in particular the Early Jurassic species *Australochelys africanus* (Gaffney & Kitching, 1995; pers. obs. BP 1/4933) and *Kayentachelys aprix* (Sterli & Joyce, 2007; Gaffney & Jenkins, 2010; pers. obs. TMM TMM 43670-2), the Early-Middle Jurassic *Condorchelys antiqua* (Sterli & de la Fuente, 2010;

Sterli et al. 2018; pers. obs. MPEF 1152, 10900) and the Middle Jurassic *Eileanchelys waldmani* (Anquetin, 2010; pers. obs. NMS G.2004.31.15), document the successive acquisition of an impedance-matching ear by the presence of an enlarged cavum tympani, a slim columella that articulates with the inferred tympanum directly, and a slim processus interfenestralis that delimits the margins of the pericapsular recess and borders the fenestra perilymphatica through which sound energy dissipates from the inner ear. *Eileanchelys waldmani* is the oldest and phylogenetically earliest branching stem-turtle that shows all osteological features of modern middle ear anatomy (pers. obs. NMS G.2004.31.15).

Several anatomical observations regarding the middle ear anatomy of fossil turtles have been published that contradict our observations, and which we interpret to be incorrect. For instance, Hetherington (2008) erroneously reported that the middle ear anatomy of some extinct crown-group turtles (*Archelon ischryos* and *Chisternon undatum* were specifically mentioned, but without specifying the species) lack the constriction and compartmentalization of extant turtles. We examined specimens of both genera (e.g. *C. undatum*: AMNH FARB 5961; *A. ischryos*: NHMW 1977/1902/001) and both have the expected middle ear anatomy consisting of a laterally positioned cavum tympani and a medially positioned cavum acustico-jugulare. Similarly, Willis et al. (2013) concluded by reference to CT scans that the middle ears of the Cretaceous fossil turtles *Galianemys emringeri*, *Galianemys whitei* and *Hamadachelys esculliciei* were openly connected to the pharynx. Phylogenetic hypotheses deeply nest these turtles within the turtle crown as pelomedusoid pleurodires (Gaffney et al. 2006). As all other crown turtles that have been studied are known to possess Eustachian tubes (Gaffney, 1979), and because the morphological features common to all extant turtles can justifiably be concluded to have been present in their common ancestor (de Queiroz & Gauthier, 1992), the observations of Willis et al. (2013) are unexpected. Instead, it is more parsimonious to assert the presence of Eustachian tubes in these fossils as well (e.g. Witmer, 1995). This conclusion is also supported by osteological correlates. The Eustachian tube typically leaves traces in the form of narrow grooves along the posterior surface of the quadrate in pleurodires (Gaffney et al. 2006) and we observed such grooves on the holotype specimens of all three species mentioned by Willis et al. (2013), for which we have CT scans. However, this osteological correlate for the Eustachian tube is not universally present in all turtles that actually have Eustachian tubes (e.g. it is absent in extant cryptodires). Therefore, the absence of this groove in the stem-group turtles, such as *P. quenstedtii* and *E. waldmani*, does not provide evidence of absence of the Eustachian tube in these taxa. Therefore, we cannot confidently infer when the Eustachian tube evolved on the turtle stem lineage.

The main middle ear structures of crown turtles appear to be relatively homogeneous across all clades. Therefore, we deduce that the ancestral turtle with a 'modern' middle ear anatomy had similar hearing abilities to its extant descendants. This habitat preference of these early extinct taxa with modern-type middle ear osteology therefore can provide information about whether the hearing apparatus of turtles evolved for hearing on land or under water. Willis et al. (2013) speculated that turtle hearing adaptively evolved in an aquatic environment because the air-filled cavum tympani appears to perform as a resonance chamber under water and because the evolution of a partitioned middle ear, with physically and acoustically uncoupled lateral and medial chambers, may improve hearing acuity under water. However, more recent, comparative data suggest that turtles across all ecological categories hear slightly better in air than under water (Christensen-Dalsgaard et al. 2012; Zeyl & Johnston, 2015). In addition, the uncoupled middle ear of mammals arose independently (Allin, 1986) on land. The available neontological evidence is therefore insufficient to conclude that the turtle ear arose in an aquatic or terrestrial environment.

As noted above, many components of the modern turtle ear arose during the Early–Middle Jurassic in the late stem lineage of turtles. The ecology of the animals documenting this transition may therefore provide evidence for the habitat in which the modern turtle ear was acquired. However, relatively little is known about the ecology of stem-turtles. This is partially because fossils of stem-turtles from the Triassic are rare, but also because different authors have published different interpretations of the available evidence. Whereas the Late Permian putative stem-turtle *Eunotosaurus africanus* shows adaptations to a fossorial lifestyle (Lyson et al. 2016), aspects of the skeletal anatomy, particularly of the gastralia/plastron of the Middle Triassic *Pappochelys rosinae* and early Late Triassic *Odontochelys semitestacea*, have been interpreted as consistent with aquatic modes of life (e.g. Rieppel, 2013; Schoch & Sues, 2017). *Odontochelys semitestacea* also has forelimb proportions consistent with those of aquatic turtles (Rieppel, 2013) and was found in marine sediments (Li et al. 2008), but the stoutness of the phalanges combined with rich associated continental fauna and flora is consistent with the possibility that *O. semitestacea* was a terrestrial animal that occasionally washed into near shore deposits (Joyce, 2015, 2017). The presence of a fully developed plastron but incomplete carapace in *O. semitestacea* has also been used as potential evidence for turtle shell evolution in an aquatic context (e.g. Rieppel & Reisz, 1999), providing hydrostatic function as ballast as well as ventral protection in an aquatic habitat (Rieppel, 2013). The ecology of some of the well-known Late Triassic stem-turtles has also been debated. *Proganochelys quenstedtii* was originally hypothesized to be similar to the extant aquatic bottom-walking species *Macrochelys temminckii*, based on gross morphology and shell

ornamentation (Gaffney, 1990). However, most lines of evidence, in particular depositional environment, shell bone histology, the presence of osteoderms, and limb morphology, suggest at present that the Late Triassic turtle *P. quenstedtii* was a terrestrial animal (Joyce & Gauthier, 2004; Scheyer & Sander, 2007; Joyce, 2015, 2017). Although shell bone histology likewise suggests a terrestrial habitat for the Late Triassic *Proterochersis robusta* (Scheyer & Sander, 2007), the shell geometry of this taxon possibly indicates a semiaquatic lifestyle instead (Benson et al. 2011). The ecologies of these early stem-group turtles are relevant to the origin of tympanic hearing and provide evidence that various habitat adaptations might have predated the evolution of the modern turtle middle ear.

As described above, most morphological changes regarding specialized middle ear anatomy of turtles appeared slightly later (and in slightly more crownward positions) on the turtle stem lineage, during the Early–Middle Jurassic. No ecological assessments have been published for *A. africanus*, which shows a deepening of the middle ear cavity, or *K. aprix*, which has an anatomically modern columella that is not articulated with the quadrate, and which also shows slight modifications to its processus interfenestralis. The Early–Middle Jurassic species *C. antiqua*, which has a middle ear anatomy approximately intermediate between *K. aprix* and *E. waldmani*, as well as *E. waldmani*, which is the first known turtle to possess a fully ‘modern’ middle ear, have shell bone histologies that have been reported to be consistent with aquatic habitat inferences (Scheyer et al. 2014; Cerda et al. 2016). Although the ecologies of *A. africanus* and *K. aprix*, which provide evidence for the earliest changes in turtle ear morphology, are unknown, the available data for *C. antiqua* and *E. waldmani* suggest that the turtle middle ear could have evolved during an aquatic stage of stem-turtle evolution. It is important to note, however, that the aquatic nature inferred for these turtles represents an amphibious lifestyle potentially similar to many extant turtles, but with an unknown degree of daily submersion.

With the exception perhaps of marine turtles and highly terrestrial tortoises, the vast majority of extant turtles likely hear on a daily basis above and under water and it is therefore perhaps not surprising that most groups hear equally well in both environments (e.g. Zeyl & Johnston, 2015). An interpretation of tympanic hearing in turtles as a versatile tool for perception of sounds in both air and water is consistent with our findings that shows only weak evolutionary changes in response to evolutionary transitions between habitats. Amphibious ecologies most likely existed during the evolution of the modern turtle middle ear along the turtle stem lineage. We therefore suggest that turtle hearing perhaps evolved as a functional compromise between the competing demands of both environments and that this arrangement is retained even in groups that predominantly inhabit one of the two realms.

Acknowledgements

We would like to express our gratitude to Patrick Campbell (NHMUK), José Carballido (MPEF), Jonah Choiniere (BP), Loic Costeur (NMB), Carl Mehling (AMNH), Mark Norell (AMNH), Linda Mogk (SMF), Alan Resetar (FMNH), Bruce Rubidge (BP), Chris Sagebiel (TMM), Rainer Schoch (SMNS), Juliana Sterli (MPEF) and Stig Walsh (NMS) for access to specimens under their care. Special thanks for Irena Raselli for the scan of *Eretmochelys* and Ingmar Werneburg for supporting this research by otherwise unpublished scans. Farah Ahmed was instrumental in scanning at NHMUK. We are furthermore indebted to Zhe-Xi Luo and April Isch Neander for generous scanning conditions and support at the University of Chicago. Jakob Christensen-Dalsgaard and Felix Quade are thanked for discussions. We thank two anonymous reviewers for their comments on an earlier draft of this work, and Anthony Graham for editing this paper. CF was supported by the Swiss National Science Foundation (grant no. 200021_156087) and German Academic Exchange Service (DAAD, no. 91546784). S.W.E. received support from an NERC studentship on the DTP Environmental Research (grant no. NE/L0021612/1) and the SYNTHESYS Project (<http://www.synthesys.info/>), which is financed by the European Community Research Infrastructure Action under the FP7 ‘Capacities’ Program. W.G.J. was supported by the Swiss National Science Foundation (grant no. 200021_156087).

References

- Adams DC (2014) A method for assessing phylogenetic least squares models for shape and other high-dimensional multivariate data. *Evolution* **68**, 2675–2688.
- Adams DC, Felice RN (2014) Assessing trait covariation and morphological integration on phylogenies using evolutionary covariance matrices. *PLoS ONE* **9**, e94335.
- Adams DC, Otarola-Castillo E (2013) geomorph: an R package for the collection and analysis of geometric morphometric shape data. *Methods Ecol Evol* **4**, 393–399.
- Allin EF (1975) Evolution of the mammalian middle ear. *J Morphol* **147**, 403–437.
- Allin EF (1986) The auditory apparatus of advanced mammal-like reptiles and early mammals. In: *The Ecology and Biology of Mammal-like Reptiles* (eds Hotton N, McLean PD, Roth JJ, Roth EC), pp. 283–294. Washington, DC: Smithsonian Institution Press.
- Anquetin J (2010) The anatomy of the basal turtle *Eileanchelys waldmani* from the Middle Jurassic of the Isle of Skye, Scotland. *Earth Env Sci Trans R Soc Edinb* **101**, 67–96.
- Anquetin J, Püntener C, Joyce WG (2017) A review of the fossil record of turtles of the clade *Thalassochelydia*. *Bull Peabody Mus Nat Hist* **58**, 31–369.
- Bapst DW (2012) paleotree: an R package for paleontological and phylogenetic analyses of evolution. *Methods Ecol Evol* **3**, 803–807.
- Bardet N, Jalil N-E, Lapparent de Broin F, et al. (2013) A giant chelonoid turtle from the Late Cretaceous of Morocco with a suction feeding apparatus unique among tetrapods. *PLoS ONE* **8**, e63586.
- Benson RBJ, Domokos G, Várkonyi PL, et al. (2011) Shell geometry and habitat determination in extinct and extant turtles (Reptilia: Testudinata). *Paleobiology* **37**, 547–562.
- Blomberg SP, Garland T, Ives AR (2003) Testing for phylogenetic signal in comparative data: behavioral traits are more labile. *Evolution* **57**, 717–745.

- Brechbühler C, Gerig G, Kübler O (1995) Parametrization of closed surfaces for 3-D shape description. *Comput Vis Image Underst* **61**, 154–170.
- Brusatte S, Benton MJ, Ruta M, et al. (2008) Superiority, competition, and opportunism in the evolutionary radiation of dinosaurs. *Science* **321**, 1485–1488.
- Cerda IA, Sterli J, Scheyer TM (2016) Bone shell microstructure of *Condorchelys antiqua* Sterli, 2008, a stem turtle from the Jurassic of Patagonia. *C R Palevol* **15**, 128–141.
- Christensen-Dalsgaard J, Brandt C, Willis KL, et al. (2012) Specialization for underwater hearing by the tympanic middle ear of the turtle, *Trachemys scripta elegans*. *Proc R Soc B* **279**, 2816–2824.
- Clack JA (1998) The neurocranium of *Acanthostega gunnari* Jarvik and the evolution of the otic region in tetrapods. *Zool J Linn Soc* **122**, 61–97.
- Clack JA (2002) Patterns and processes in the early evolution of the tetrapod ear. *J Neurobiol* **53**, 251–264.
- Clack JA, Allin E (2004) The evolution of single-and multiple-ossicle ears in fishes and tetrapods. *Springer Handbook Aud Res* **22**, 128–163.
- Clack JA, Anderson JA (2017) Early tetrapods: experimenting with form and function. In: *Evolution of the Vertebrate Ear: Evidence from the Fossil Record* (eds Clack JA, Fay RR, Popper AN), pp. 71–105. Cham: Springer Nature.
- Clack JA, Fay RR, Popper AN (2016) *Evolution of the Vertebrate Ear. Evidence from the Fossil Record*. Cham: Springer Nature.
- Claude J, Paradis E, Tong H, et al. (2003) A geometric morphometric assessment of the effects of environment and cladogenesis on the evolution of the turtle shell. *Biol J Linn Soc* **79**, 485–501.
- Colafrancesco KC, Gridi-Papp M (2016) Vocal sound production and acoustic communication in amphibians and reptiles. *Springer Handbook Aud Res* **53**, 51–82.
- Coleman MN, Colbert MW (2010) Correlations between auditory structures and hearing sensitivity in non-human primates. *J Morphol* **271**, 511–532.
- Curtis AA, Van Valkenburgh B (2014) Beyond the sniffer: frontal sinuses in Carnivora. *Anat Rec* **297**, 2047–2064.
- de Queiroz K, Gauthier J (1992) Phylogenetic taxonomy. *Annu Rev Ecol Syst* **23**, 449–480.
- Domokos G, Várkonyi PL (2008) Geometry and selfrighting of turtles. *Proc R Soc B* **275**, 11–17.
- Ekdale EG (2016) Form and function of the mammalian inner ear. *J Anat* **228**, 324–337.
- Evans SE (2017) The lepidosaurian ear: variations on a theme. In: *Evolution of the Vertebrate Ear: Evidence from the Fossil Record* (eds Clack JA, Fay RR, Popper AN), pp. 245–284. Cham: Springer Nature.
- Evers SW (2019) Project: Evers 2019, CT scans of extant turtle skulls. MorphoSource. Available at https://www.morphosource.org/Detail/ProjectDetail/Show/project_id/769.
- Evers SW, Benson RBJ (2018) Project: Evers & Benson 2018, Turtle CT data and 3D models. MorphoSource. Available at http://www.morphosource.org/Detail/ProjectDetail/Show/project_id/462.
- Evers SW, Benson RBJ (2019) A new phylogenetic hypothesis of turtles with implications for the timing and number of evolutionary transitions to marine lifestyles in the group. *Palaeontology* **62**, 93–134.
- Evers SW, Barrett PM, Benson RBJ (2019) Anatomy of *Rhinochelys pulchriiceps* (Protostegidae) and marine adaptation during the early evolution of chelonoids. *PeerJ* **7**, e6811.
- Felsenstein J (1985) Confidence limits on phylogenies with a molecular clock. *Syst Biol* **34**, 152–161.
- Ferreira GS, Werneburg I (2019) Evolution, diversity, and development of the craniocervical system in turtles with special reference to jaw musculature. In: *Heads, Jaws, and Muscles* (eds Ziermann JM, Diaz RE, Diogo R), pp. 171–206. Berlin: Springer.
- Foth C, Joyce WG (2016) Slow and steady: cranial disparity through time in fossil and recent turtles. *Proc R Soc B* **283**, 20161881.
- Foth C, Rabi M, Joyce WG (2017) Skull shape variation in recent and fossil Testudinata and its relation to habitat and feeding ecology. *Acta Zool* **98**, 310–325.
- Gaffney ES (1975) *Solnhofia parsoni*, a new cryptodiran turtle from the Late Jurassic of Europe. *Am Mus Novit* **2576**, 1–25.
- Gaffney ES (1976) Cranial morphology of the European Jurassic turtles *Portlandemys* and *Plesiochelys*. *Bull Am Mus Nat Hist* **157**, 488–543.
- Gaffney ES (1979) Comparative cranial morphology of recent and fossil turtles. *Bull Am Mus Nat Hist* **164**, 65–376.
- Gaffney ES (1990) The comparative osteology of the Triassic turtle *Proganochelys*. *Bull Am Mus Nat Hist* **194**, 1–263.
- Gaffney ES, Jenkins FA (2010) The cranial morphology of *Kayentachelys*, an early Jurassic cryptodire, and the early history of turtles. *Acta Zool* **91**, 335–368.
- Gaffney ES, Kitching JW (1995) The morphology and relationships of *Australochelys*, an early Jurassic turtle from South Africa. *Am Mus Novit* **3130**, 1–29.
- Gaffney ES, Tong H, Meylan PA (2006) Evolution of the side-necked turtles: the families Bothremyidae, Euraxemyidae, and Araripemyidae. *Bull Am Mus Nat Hist* **300**, 1–318.
- Garland T, Ives AR (2000) Using the past to predict the present: confidence intervals for regression equations in phylogenetic comparative methods. *Am Nat* **155**, 346–364.
- Grafen A (1989) The phylogenetic regression. *Philos Trans R Soc Lond B Biol Sci* **326**, 119–157.
- Hammer Ø, Harper DAT, Ryan PD (2001) PAST: paleontological Statistics software package for education and data analysis. *Palaeontol Electron* **4**, 1–9.
- Henson OW (1974) Comparative anatomy of the middle ear. In: *Handbook of Sensory Physiology, Vol. V-I, Auditory System* (eds Keidel WD, Neffs WD), pp. 39–110. New York: Springer-Verlag.
- Hetherington T (2008) Comparative anatomy and function of hearing in aquatic amphibians, reptiles, and birds. In: *Sensory Evolution on the Threshold: Adaptations in Secondarily Aquatic Vertebrates* (eds Thewissen JGM, Nummela S), pp. 183–209. Berkeley: University of California Press.
- Iverson JB, Le M, Ingram C (2013) Molecular phylogenetics of the mud and musk turtle family Kinosternidae. *Mol Phylogenet Evol* **69**, 929–939.
- Jackson DA (1993) Stopping rules in principal components analysis: a comparison of heuristical and statistical approaches. *Ecology* **74**, 2204–2214.
- Jones MEH, Werneburg I, Curtis N, et al. (2012) The head and neck anatomy of sea turtles (Cryptodira: Cheloniodea) and skull shape in Testudines. *PLoS ONE* **7**, e47852.
- Joyce WG (2007) Phylogenetic relationships of Mesozoic turtles. *Bull Peabody Mus Nat Hist* **48**, 3–102.
- Joyce WG (2015) The origin of turtles: a paleontological perspective. *J Exp Zool B* **324**, 181–193.

- Joyce WG (2017) A review of the fossil record of basal Mesozoic turtles. *Bull Peabody Mus Nat Hist* **58**, 65–113.
- Joyce WG, Gauthier JA (2004) Palaeoecology of Triassic stem turtles sheds new light on turtle origins. *Proc R Soc B* **271**, 1–5.
- Joyce WG, Parham JF, Lyson TR, et al. (2013) A divergence dating analysis of turtles using fossil calibrations: an example of best practices. *J Paleontol* **87**, 612–634.
- Joyce WG, Rabi M, Clark JM, et al. (2016) A toothed turtle from the Late Jurassic of China and the global biogeographic history of turtles. *BMC Evol Biol* **16**, 236.
- Kardong KV (2012) *Vertebrates: Comparative Anatomy, Function, Evolution*. 6th edn. New York: McGraw-Hill.
- Lapparent de Broin F, Bardet N, Amaghaz M, et al. (2014) A strange new chelonoid turtle from the latest cretaceous phosphates of Morocco. *C R Palevol* **13**, 87–95.
- Lautenschlager S, Ferreira GS, Werneburg I (2018) Sensory evolution and ecology of early turtles revealed by digital endocranial reconstructions. *Front Ecol Evol* **6**, 1–16.
- Lavender AL, Bartol SM, Bartol IK (2014) Ontogenetic investigation of underwater hearing capabilities in loggerhead sea turtles (*Caretta caretta*) using a dual testing approach. *J Exp Biol* **217**, 2580–2589.
- Le M, McCord WP (2008) Phylogenetic relationships and biogeographical history of the genus *Rhinoclemmys* Fitzinger, 1835 and the monophyly of the turtle family Geoemydidae (Testudines: Testudinoidea). *Zool J Linn Soc* **153**, 751–767.
- Le M, Duong HT, Dinh LD, et al. (2014) A phylogeny of softshell turtles (Testudines: Trionychidae) with reference to the taxonomic status of the critically endangered, giant softshell turtle, *Rafetus swinhoei*. *Org Divers Evol* **14**, 279–293.
- Legoux JP, Wisner A (1955) Rôle fonctionnel des bulles tympaniques géantes de certains rongeurs (Meriones). *Acustica* **5**, 208–216.
- Lenhardt ML, Klinger RC, Musick JA (1985) Marine turtle middle-ear anatomy. *J Aud Res* **25**, 66–72.
- Li C, Wu X-C, Rieppel O, et al. (2008) An ancestral turtle from the Late Triassic of south-western China. *Nature* **456**, 497–501.
- Lombard RE, Bolt JR (1979) Evolution of the tetrapod ear: an analysis and reinterpretation. *Biol J Linn Soc* **11**, 19–76.
- Lourenço JM, Claude J, Galtier N, et al. (2012) Dating cryptodiran nodes: origin and diversification of the turtle superfamily Testudinoidea. *Mol Phylogenet Evol* **62**, 496–507.
- Luo ZX, Schultz JA, Ekdale EG (2016) Evolution of the middle and inner ears of mammaliaforms: the approach to mammals. *Springer Handbook Aud Res* **59**, 139–174.
- Lyson TR, Rubidge BS, Scheyer TM, et al. (2016) Fossorial origin of the turtle shell. *Curr Biol* **26**, 1–8.
- Manley GA (1972) A review of some current concepts of the functional evolution of the ear in terrestrial vertebrates. *Evolution* **26**, 608–621.
- Mason MJ (2016) Structure and function of the mammalian middle ear. I: large middle ears in small desert mammals. *J Anat* **228**, 284–299.
- McPeck MA, Shen L, Farid H (2009) The correlated evolution of three-dimensional reproductive structures between male and female damselflies. *Evolution* **63**, 73–83.
- McPeck MA, Symes LB, Zong DM, et al. (2011) Species recognition and patterns of population variation in the reproductive structures of a damselfly genus. *Evolution* **65**, 419–428.
- Moore WJ (1981) *The Mammalian Skull*, vol. 8. Cambridge: Cambridge University Press.
- Motani R, Schmitz L (2011) Phylogenetic functional signals in the evolution of form-function relationships in terrestrial vision. *Evolution* **65**, 2245–2257.
- Müller J, Tsuji LA (2007) Impedance-matching hearing in Paleozoic reptiles: evidence of advanced sensory perception at an early stage of amniote evolution. *PLoS ONE* **2**, e889.
- Nummela S, Thewissen JGM (2008) The physics of sound in air and water. In: *Sensory Evolution on the Threshold: Adaptations in Secondarily Aquatic Vertebrates* (eds Thewissen JGM, Nummela S), pp. 175–181. Berkeley: University of California Press.
- Olson EC (1966) The middle ear – morphological types in amphibians and reptiles. *Am Zool* **6**, 399–419.
- Pagel MD (1997) Inferring evolutionary processes from phylogenies. *Zool Scripta* **26**, 331–348.
- Pagel MD (1999) Inferring the historical patterns of biological evolution. *Nature* **401**, 877–884.
- Paradis E, Claude J, Strimmer K (2004) APE: analysis of phylogenetics and evolution in R language. *Bioinformatics* **20**, 289–290.
- Pereira AG, Sterli J, Moreira FPP, et al. (2017) Multilocus phylogeny and statistical biogeography clarify the evolutionary history of major lineages of turtles. *Mol Phylogenet Evol* **113**, 59–66.
- Pinheiro J, Bates D, DebRoy S, et al. (2018) *nlme: Linear and Nonlinear Mixed Effects Models. R package version 3.1*, p. 137. <https://cran.r-project.org/>
- Piniak WED, Mann DA, Eckert SC, et al. (2016) Amphibious hearing in sea turtles. *Adv Exp Med Biol* **730**, 83–87.
- Polly PD, Stayton CT, Dumont ER, et al. (2016) Combining geometric morphometrics and finite element analysis with evolutionary modeling: toward a synthesis. *J Vertebr Paleontol* **36**, e1111225.
- Raselli I (2018) Comparative cranial morphology of the Late Cretaceous protostegid sea turtle *Desmatochelys lowii*. *PeerJ* **6**, e5964.
- Renous S, de Lapparent de Broin F, Depecker M, et al. (2008) Evolution of locomotion in aquatic turtles. In: *Biology of Turtles* (eds Wyneken J, Godfrey MH, Bels V), pp. 97–138. Boca Raton: CRC Press.
- Revell LJ (2009) Size-correction and principal components for interspecific comparative studies evolution. *Evolution* **63**, 3258–3268.
- Revell LJ (2012) phytools: an R package for phylogenetic comparative biology (and other things). *Methods Ecol Evol* **3**, 217–223.
- Ridgway H, Wever EG, McCormick JG, et al. (1969) Hearing in the giant sea turtle, *Chelonia mydas*. *PNAS* **64**, 884–890.
- Rieppel O (2013) The evolution of the turtle shell. In: *Morphology and Evolution of Turtles* (eds Brinkman DB, Holroyd PA, Gardner JD), pp. 51–61. Berlin: Springer.
- Rieppel O, Reisz RR (1999) The origin and early evolution of turtles. *Annu Rev Ecol Evol Syst* **30**, 1–22.
- Ritchie DW, Kemp GL (1999) Fast computation, rotation, and comparison of low resolution spherical harmonic molecular surfaces. *J Comput Chem* **20**, 383–395.
- Rohlf FJ (2001) Comparative methods for the analysis of continuous variables: geometric interpretations. *Evolution* **55**, 2143–2160.
- Rohlf FJ, Corti M (2000) Use of two-block partial least-squares to study covariation in shape. *Syst Biol* **49**, 740–753.

- Rosowski JJ (1992) Hearing in transitional mammals: predictions from the middle ear anatomy and hearing capabilities of extant mammals. In: *The Evolutionary Biology of Hearing* (eds Webster DB, Fay RR, Popper AN), pp. 615–631. New York: Springer.
- Rosowski JJ, Graybeal A (1991) What did *Morganucodon* hear? *Zool J Linn Soc* **101**, 131–168.
- Saunders JC, Duncan RK, Doan DE, et al. (2000) The middle ear of reptiles and birds. *Springer Handbook Aud Res* **13**, 13–69.
- Scheyer TM, Sander PM (2007) Shell bone histology indicates terrestrial palaeoecology of basal turtles. *Proc R Soc B* **274**, 1885–1893.
- Scheyer TM, Danilov DG, Sukhanov VB, et al. (2014) The shell bone histology of fossil and extant marine turtles revisited. *Biol J Linn Soc* **112**, 701–718.
- Schmitz L, Motani R (2011) Nocturnality in dinosaurs inferred from scleral ring and orbit morphology. *Science* **332**, 705–708.
- Schoch RR, Sues H-D (2017) Osteology of the Middle Triassic stem-turtle *Pappochelys rosinae* and the early evolution of the turtle skeleton. *J Syst Palaeontol* **16**, 927–965.
- Shen L, Makedon F (2006) Spherical mapping for processing of 3D closed surfaces. *Image Vis Comput* **24**, 743–761.
- Shen L, Farid H, McPeck MA (2009) Modeling three-dimensional morphological structures using spherical harmonics. *Evolution* **63**, 1003–1016.
- Sobral G, Reisz R, Neenan JM, et al. (2016) Basal reptilians, marine diapsids, and turtles: the flowering of reptile diversity. *Springer Handbook Aud Res* **59**, 207–243.
- Spinks PQ, Thomson RC, McCartney-Melstad E, et al. (2016) Phylogeny and temporal diversification of the New World pond turtles (Emydidae). *Mol Phylogenet Evol* **103**, 85–97.
- Spoor F, Zonneveld F (1998) Comparative review of the human bony labyrinth. *Am J Phys Anthropol* **41**, 211–251.
- Sterli J, de la Fuente MS (2010) Anatomy of *Condorchelys antiqua* Sterli, 2008, and the origin of the modern jaw closure mechanism in turtles. *J Vertebr Paleontol* **30**, 351–366.
- Sterli J, Joyce WG (2007) The cranial anatomy of the Early Jurassic turtle *Kayentachelys aprix*. *Acta Palaeontol Pol* **52**, 675–694.
- Sterli J, de la Fuente MS, Rougier GW (2018) New remains of *Condorchelys antiqua* (Testudinata) from the Early-Middle Jurassic of Patagonia: anatomy, phylogeny, and paedomorphosis in the early evolution of turtles. *J Vertebr Paleontol* **38**, e1480112.
- Tong H, Meylan PA (2013) Morphology and relationships of *Brachyopsemys tingitana* gen. et sp. nov. from the Early Paleocene of Morocco and recognition of the new eucryptodiran turtle family: Sandownidae. In: *Morphology and Evolution of Turtles* (eds Brinkman DB, Holroyd PA, Gardner JD), pp. 187–212. Berlin: Springer.
- Vargas-Ramírez M, Castaño-Mora OV, Fritz U (2008) Molecular phylogeny and divergence times of ancient South American and Malagasy river turtles (Testudines: Pleurodira: Podocnemididae). *Org Divers Evol* **8**, 388–398.
- Webster DB, Webster M (1975) Auditory systems of Heteromyidae: functional morphology and evolution of the middle ear. *J Morphol* **146**, 343–376.
- Weems RE, Brown KM (2017) More-complete remains of *Procolpochelys charlestonensis* (Oligocene, South Carolina), an occurrence of *Euclastes* (upper Eocene, South Carolina), and their bearing on Cenozoic pancheloniid sea turtle distribution and phylogeny. *J Paleontol* **91**, 1228–1243.
- Werneburg I (2011) The cranial musculature of turtles. *Palaeontol Electron* **14**, 15a.
- Werneburg I (2013) Jaw musculature during the dawn of turtle evolution. *Org Divers Evol* **13**, 225–254.
- Werneburg I (2015) Neck motion in turtles and its relation to the shape of the temporal skull region. *C R Palevol* **14**, 527–548.
- Wever EG (1978) *The Reptile Ear: Its Structure and Function*. Princeton: Princeton University Press.
- Willis KL, Christensen-Dalsgaard J, Ketten DR, et al. (2013) Middle ear cavity morphology is consistent with an aquatic origin for testudines. *PLoS ONE* **8**, e54086.
- Witmer LM (1995) The extant phylogenetic bracket and the importance of reconstructing soft tissues in fossils. In: *Functional Morphology in Vertebrate Paleontology* (ed. Thompson JJ), pp. 19–33. Cambridge: Cambridge University Press.
- Zelditch ML, Swiderski DL, Sheets HD (2012) *Geometric Morphometrics for Biologists: A Primer*. Amsterdam: Elsevier Academic Press.
- Zeyl JN, Johnston CE (2015) Amphibious auditory evoked potentials in four North American Testudines genera spanning the aquatic–terrestrial spectrum. *J Comp Physiol A* **201**, 1011–1018.

Supporting Information

Additional Supporting Information may be found in the online version of this article:

Table S1. Specimens used in this study and CT data repository information.

Table S2. Morphometric measurements of turtle skulls and middle ears, habitat preferences, and values for the first four PCs.

Table S3. All results of the phylogenetic generalized least square (pGLS) regression analyses.

Table S4. All PCs generated from the SPHARM analyses.

Table S5. Results of phylogenetic flexible discriminant analyses (pFDA) exploring shape of the lateral middle ear cavity compared with habitat preferences for morphometric measurements and principal components.

Table S6. Results of the D.pGLS testing ecological constraints (Forelimb1 to Forelimb6) for middle ear measurements and shape.

Appendix S1. Additional supporting tables

Appendix S2. R code for calculating morphometric measurements of the middle ear using landmarks placed around the perimeters of the tympanic recess and the fenestra ovalis

Appendix S3. Nexus file of phylogenetic tree

Appendix S4. 3D PDF showing the shape variation of PC1 to PC4 based on the SPHARM analyses

Appendix S5. Results of the two-block partial least squares regression analysis of shape and size parameters against skull box